



**Structurally-modified subphthalocyanines: molecular design
towards realization of expected properties from its
electronic structure and structural features**

Journal:	<i>ChemComm</i>
Manuscript ID:	CC-FEA-02-2014-001526
Article Type:	Feature Article
Date Submitted by the Author:	28-Feb-2014
Complete List of Authors:	Shimizu, Soji; Tohoku University, Graduate School of Science Kobayashi, Nagao; Tohoku University, Department of Chemistry, Graduate School of Science

FEATURE ARTICLE

Structurally-modified subphthalocyanines: molecular design towards realization of expected properties from its electronic structure and structural features

Cite this: DOI: 10.1039/x0xx00000x

Received 00th January 2012,
Accepted 00th January 2012

DOI: 10.1039/x0xx00000x

www.rsc.org/

Soji Shimizu* and Nagao Kobayashi*

This feature article summarizes recent contributions of the authors in the synthesis of structurally-modified subphthalocyanines, which cover (1) modification of the conjugated system of subphthalocyanine to create novel conjugated systems comprising three pyrroles or pyrrole-like subunits, (2) core-modification by expansion of the inner pyrrolic five-membered ring to larger six- and seven-membered ring units, and (3) exterior-modification by annulation of functional units to subphthalocyanine. These modifications on the structure of subphthalocyanine have been performed with the aim of demonstrating unique properties originating from the bowl-shaped C_{3v} -symmetric structure as well as the electronic structure delineated by the 14π -electron conjugated system on the curved molecular surface. The possible structural modifications surveyed in this feature article and their concomitant properties will provide an important future guide to the design of subphthalocyanine-based functional molecules, considering the fact that subphthalocyanine has recently been attracting considerable attention as a potential candidate in the fields of the optoelectronics and molecular electronics.

1. Introduction

Subphthalocyanine (SubPc **1**)¹ is the sole contracted analogue of phthalocyanine (Pc **2**): “*sub*” refers to any conjugated macrocycles containing three pyrrole or pyrrole-like subunits, and “*contracted analogue*” represents macrocycles with smaller numbers of π -electrons in the conjugation framework as compared to the 18π -electrons of porphyrins or Pc (Fig. 1).² The first synthesis of this unique contracted molecule can be traced back to 1972 during the synthetic trial of a boron complex of Pc by Meller and Ossko using boron trichloride, the templating effect of which accidentally led to the generation of SubPc as a cyclotrimerization product of *o*-phthalonitrile.³

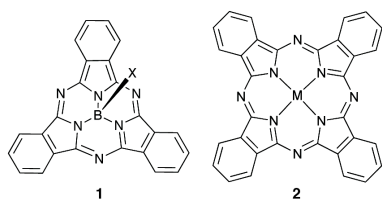


Fig. 1. Subphthalocyanine (SubPc **1**) and phthalocyanine (Pc **2**).

SubPc generally exhibits vivid pink-to-purple colours as complimentary colours of its Soret and Q band absorptions in the UV and visible regions and moderately intense fluorescence with quantum yields ranging from 0.2 to 0.5,⁴ both of which are characteristic of its electronic structure delineated by the macrocyclic 14π -electron conjugated system.¹ Another unique feature of SubPc lies in its bowl-shaped molecular structure arising from the steric demand of arranging three isoindole units around the central boron atom. These optical properties as well as the structural features have promoted this *contracted sub*-species of Pc into the class of singular functional molecules with possible applications in the fields of optoelectronics and molecular electronics.^{1,5-9} Furthermore, the research interests in this molecule has been enhanced since SubPc has been the only available *sub*-species not only in phthalocyanine chemistry, but also in porphyrin chemistry until the recent successive synthetic achievements of subporphyrins and related analogues by the groups of Osuka,¹⁰ Latos-Grażyński,¹¹ Shen, Yamada,¹² and Kobayashi¹³ (Fig. 2, 3-7).

In addition to its potential application as a functional dye, the following research interests stemming from the above-mentioned unique features and properties have been centred in investigations into the chemistry of SubPc: (1) possible tuning

of the absorption and fluorescence of SubPc by perturbing its conjugated system, (2) aromaticity arising from the convex and concave surfaces of the bowl-shaped SubPc structure, and (3) three-dimensional chirality, which can be more intuitively referred to as “bowl-chirality”.¹⁴ Most of these topics have been pioneered by Torres *et al.* and our group using genuine SubPc or simply modified species in most of the previous investigations reported by these two groups.¹ In order to further pursue these research interests, structural modifications have become the next important research direction, which has motivated us to carry out possible modifications of the structure of SubPc.

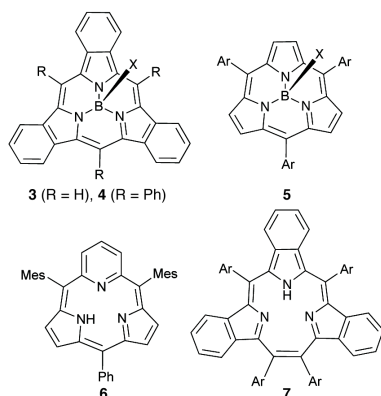


Fig. 2. Subporphyrin and related analogues: tribenzosubporphine **3**, meso-aryl-substituted tribenzosubporphine **4**, meso-aryl-substituted subporphyrin **5**, subpyrroloporphyrin **6**, and [14]triphyrin(2.1.1) **7**.

SubPc comprises three isoindole units bridged by imino-nitrogen atoms. A possible modification is, therefore, performed on the isoindole units or on its bridging units. The former is, further, separated into modifications of the inner pyrrolic five-membered ring and the exterior benzo moiety, which are referred to as *core-modification* and *exterior-modification*, respectively, in this manuscript (Fig. 3). In this feature article, these possible structural modifications surveyed in the course of our research of SubPc are documented. In addition, the optical and electrochemical properties of the structurally-modified SubPcs, which relate to the above-mentioned research interests, are also clearly described based on spectroscopic measurements and theoretical calculations.

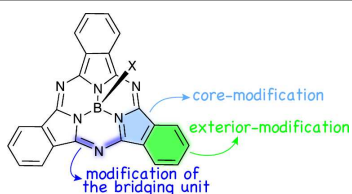


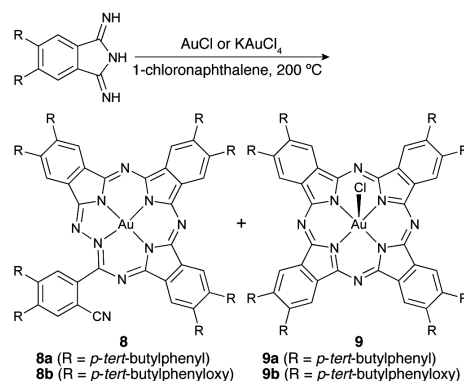
Fig. 3. Possible modifications of the structure of SubPc.

2. Modification of the bridging unit – a triphyrin structure with a novel conjugated system

Difficulty in replacing the imino-nitrogen bridges of SubPc by other bridging units is easily conceivable considering that

SubPc can only be synthesized by cyclotrimerization reaction of *o*-phthalonitrile derivatives, and an efficient stepwise synthesis using precursors with fragmentary structures of SubPc as building blocks has not yet been available.¹ This synthetic limitation is in marked contrast to the synthesis of subporphyrins and its analogues. For example, subpyrroloporphyrin **6** was synthesized in a stepwise manner by macrocyclization of a linear bispyrrolylmethylpyridine precursor,¹¹ whereas a [14]triphyrin(2.1.1) structure, initially synthesized serendipitously during the synthesis of meso-aryl-substituted porphyrin from a pyrrole derivative with a bicyclo[2.2.2]octadiene unit by Shen and Yamada,¹² could be recently synthesized by McMurry coupling reaction of a tripyrrole precursor bearing formyl groups at the terminal α -positions¹⁵ or acid-catalyzed reaction of arylaldehyde and dipyrroloethene.¹⁶ Recently Osuka *et al.* successfully achieved the synthesis of an A₂B-type subporphyrin using a boron complex of tripyrrane as a synthetic intermediate.¹⁷

Instead of using synthetic precursors, an alternative template from boron will possibly generate the target SubPc analogues with a different bridging unit. Although substitution of the central boron atom with other elements, such as Al, Ga, C, Si, Ge, and Mg, has been theoretically investigated,¹⁸ it still remains a challenge to find another suitable template for the formation of a triphyrin structure in phthalocyanine chemistry. During the course of our re-investigation of a gold complex of Pc, which was preliminary reported in 1965,¹⁹ we serendipitously isolated a novel SubPc analogue **8** along with a gold(III) complex of Pc **9** (Scheme 1).²⁰



Scheme 1. Synthesis of gold complex of [18]tribenzo-pentaazatriphyrin(4.1.1) **8** and gold complex of Pc **9**.

Based on the X-ray crystal structural analysis, **8** comprises of an *aza*-triphyrin structure bridged by a unique N-C-N-N linkage, in which the central gold(III) ion is coordinated by the three isoindole units and one of the nitrogen atoms of the bridging unit (Fig. 4). The bonding pattern in the structure of **8** demonstrates its 18 π -electron conjugated system. According to the conventional nomenclature of porphyrinoids,²¹ this macrocycle can be referred to as [18]tribenzo-pentaazatriphyrin(4.1.1). In this nomenclature, the numbers in the brackets and parentheses indicate the number of π -electrons and bridging atoms, respectively.

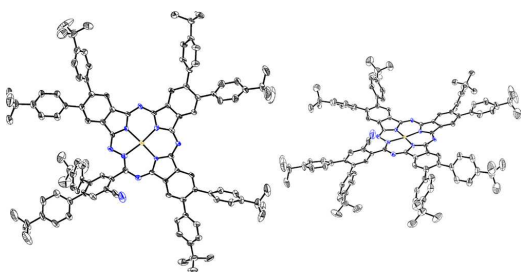


Fig. 4. X-ray single crystal structure of gold complex of [18]tribenzo-pentaazatriphyrin(4.1.1) **8a**, top view (left) and side view (right). The thermal ellipsoids were scaled to the 50% probability level. Hydrogen atoms were omitted for clarity (Reproduced from Ref. 20 with permission from Wiley).

As a gold source, either gold(I) chloride or potassium tetrachloroaurate(III) can be utilized to synthesize both **8** and **9** (Scheme 1). Since a gold(I) ion is easily oxidized to a gold(III) ion, a gold(III) ion is plausibly the actual templating species. Although the reaction mechanism to provide **8** is still unclear, the unique template effects of the gold(III) ion, such as a square planar coordination geometry and its relatively large ion size, may hinder cyclotetramerization towards a Pc structure rather than generate the more favourable structure of **8** by reacting three and half 1,3-diiminoisoindolines, which was evidenced by regeneration of the cyano group from the 1,3-diiminoisoindoline.

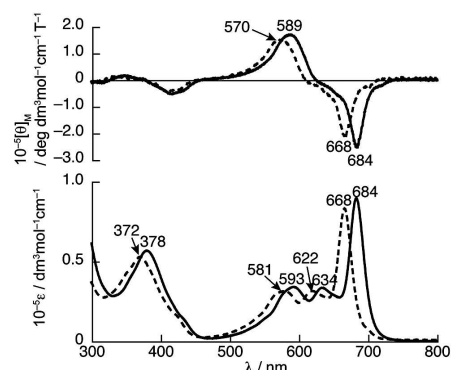


Fig. 5. UV/Vis absorption (bottom) and MCD (top) spectra of **8a** (solid line) and **8b** (dashed line) in toluene (Reproduced from Ref. 20 with permission from Wiley).

The absorption spectrum of **8** showed Soret and Q band absorptions, which are typical absorptions for porphyrinoids with a macrocyclic conjugated system (Fig. 5). The allowed Soret band absorption and forbidden Q band absorption generally observed for porphyrins are interpreted in terms of Gouterman's four orbital model as a theoretical framework, in which these absorptions originate from transitions from nearly degenerate HOMO (HOMO and HOMO-1) to degenerate LUMO (LUMO and LUMO+1) and their configuration interactions.²² In the case of Pc, near degeneracy of the HOMO and HOMO-1 seen in normal porphyrinoids turn to non-degenerate due to the electron-withdrawing effect of nitrogen atoms at the *meso*-positions, so that the forbidden nature of the Q band absorptions is reduced, leading to an intense Q band absorption of Pc analogues.²³ **8** similarly exhibited an intense Q

band absorption (**8a**: 684 nm, **8b**: 668 nm) with two shoulder-like bands (**8a**: 634 and 593 nm, **8b**: 622 and 581 nm). This spectral morphology is, therefore, indicative of a Pc-like 18 π -electron conjugated system for **8**.

Magnetic circular dichroism (MCD) spectroscopy, which is an invaluable spectroscopic technique for probing the electronic structures of porphyrinoids, generally provides characteristic MCD spectral patterns called Faraday *A* and *B* terms corresponding to the Soret and Q band absorptions.²³⁻²⁵ Faraday *A* term, a derivative-shaped signal with an inflection point at the absorption maximum, is generally observed when the excited states are orbitally degenerate, whereas Faraday *B* terms, a set of trough and peak with gaussian-type shapes corresponding closely to the absorption maxima, are observed for magnetically-coupled non-degenerate absorptions when the excited states are non-degenerate (Fig. 6). As the Soret and Q band absorptions of porphyrinoids are interpreted based on Gouterman's four orbital model, Faraday *A* and *B* terms corresponding to these bands are indicative of degeneracy and non-degeneracy of the LUMO and LUMO+1, respectively. Moreover, MCD signals corresponding to the Soret and Q band absorptions change from minus to plus in ascending energy when $\Delta\text{HOMO} > \Delta\text{LUMO}$, and from plus to minus when $\Delta\text{HOMO} < \Delta\text{LUMO}$, where ΔHOMO and ΔLUMO are energy differences between the HOMO and HOMO-1 and between the LUMO and LUMO+1, respectively. Analysis of the electronic structures of Pc and related analogues based on this spectroscopic technique, therefore, enables explicit assignment of the positions of the Soret and Q band absorptions and provides information about orbital degeneracy of the excited states and relative energy differences of the four frontier orbitals.

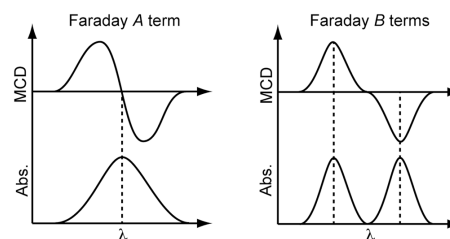


Fig. 6. Schematic representation of Faraday *A* term and Faraday *B* terms in the MCD spectroscopy.

The MCD spectrum of **8** exhibited a negative-to-positive sequence of MCD signals in ascending energy with respect to the intense Q band (**8a**: 684 nm, **8b**: 668 nm) and one of the shoulder-like bands (**8a**: 593 nm, **8b**: 581 nm, Fig. 5). These MCD signals in the Q band region are typical Faraday *B* terms, hence indicating non-degeneracy of the LUMO and LUMO+1 of **8**. The band assignment and frontier molecular orbital (MO) diagram as inferred from the MCD spectroscopic results was further evidenced by DFT and time-dependent DFT (TDDFT) calculations. In the MO diagram, a significant energy difference of the LUMO and LUMO+1 was estimated due to the low molecular symmetry of **8** (Fig. 7). Based on these results, we can conclude that the electronic structure of **8** is mainly

delineated by a Pc-like 18π -electron conjugated system,²⁶ and that the structural perturbation due the low symmetric triphyrin-like structure causes broadening of the Q band absorption.

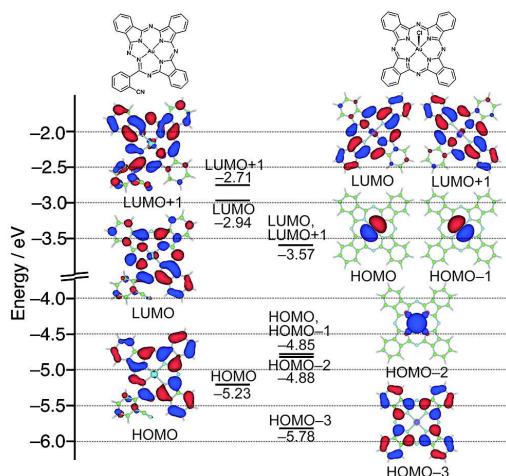
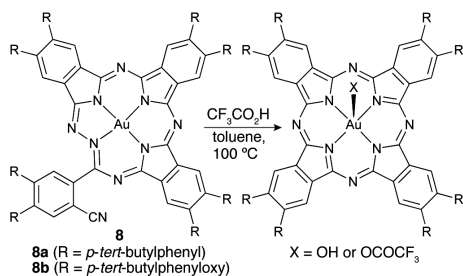


Fig. 7. Partial frontier MO diagrams of **8** (left) and **9** (right). The model structures used for the calculation are shown above (Reproduced from Ref. 20 with permission from Wiley).

In addition to its unique structure, **8** also exhibited an unusual ring-expansion reactivity to **9** under acidic conditions. **8** can be converted into **9** in moderate yields (41% in the case of **8b**) in toluene at 100 °C in the presence of trifluoroacetic acid (Scheme 2). Although the mechanism of this thermal interconversion from **8** to **9** is still uncertain, the protonation-induced ring-expansion from the triphyrin to Pc infers that **8** is a kinetic product in the ring-formation reaction of Pc, which is more plausibly stabilized by coordination of the gold(III) ion.



Scheme 2. Protonation-induced ring-expansion reaction of **8**.

3. Core-modification – SubPc analogues with an expanded ring unit in the core

Core-modification, replacement of pyrrole or isoindole units in the structures of porphyrin and Pc by other heterocycles, has been more frequently investigated in the chemistry of porphyrins than in that of Pcs.²⁷ This is mainly due to the easy availability of the corresponding precursors for the synthesis of core-modified porphyrins and the facile synthesis of porphyrin analogues in a stepwise manner. Although the stepwise synthetic reaction of subporphyrins has still been fairly limited, recently Latos-Grażyński *et al.* succeeded in applying this core-modification strategy of porphyrins to the synthesis of the first

core-modified subporphyrin, subpyrriporphyrin **6**,¹¹ in which one of the pyrrole rings is replaced by a pyridine ring (Fig. 2). This is also the first example of the synthesis of *sub*-species without using a boron template, which had been indispensable in the syntheses of both subporphyrin and SubPc. In contrast to porphyrin chemistry, core-modified Pc analogues have been fairly rare, except for hemiporphyrazines **10** (Fig. 8).²⁸⁻³⁰ Hemiporphyrazine can be easily synthesized from a mixed-condensation reaction of 1,3-diminoisoindoline and heterocyclic diamines. As the bite angles between the amines determine the size of the resulting macrocycles, not only the [2+2]-type hemiporphyrazines but also [3+3]-type hemiporphyrazines **11** can be synthesized.^{31,32} Although the formation of aromatic hemiporphyrazine was recently achieved by introducing hydroxy and ketone groups to the *meta*-positions of the *meta*-phenylene moieties of hemiporphyrazine **12**,³³ hemiporphyrazines are basically non-aromatic due to the predominant local conjugation of the embedded aromatic ring units rather than the macrocyclic conjugation. Core-modification without any loss of aromaticity and macrocyclic conjugation has, therefore, remained a challenge in the chemistry of Pcs.

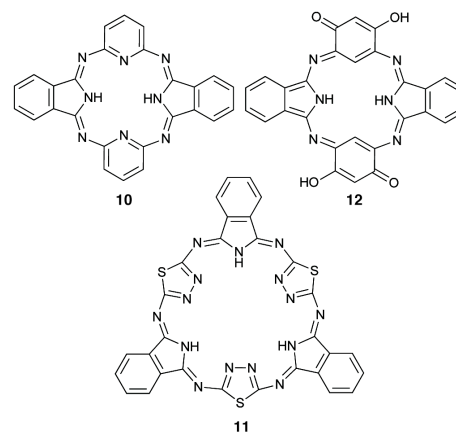


Fig. 8. Representative hemiporphyrazines **10-12**.

Recently we succeeded in synthesizing of core-modified Pc analogues **13-15**, which retain Pc-like 18π -like conjugated systems, using dinitrile precursors bearing cyano groups at positions with a 1,3- or 1,4-relationship, such as 1,8-naphthalenedicarbonitrile or 2,2'-biphenyldicarbonitrile (Fig. 9).³⁴ This synthetic strategy is based on the idea that the five-membered pyrrole ring of the isoindole moiety of Pc originates from a 1,2-relationship of the position of cyano groups in *o*-phthalonitrile, which is a precursor of Pc. The same strategy was, then, applied to the synthesis of SubPc, and a six-membered pyridine unit and seven-membered azepine unit were successfully introduced in the place of the five-membered pyrrole ring unit in SubPc (Scheme 3).^{35,36} In addition to the properties in line with the corresponding core-modified Pc analogues **13-15**,³⁴ the embedded larger ring units in SubPc result in unique properties, which are described in the following sections.

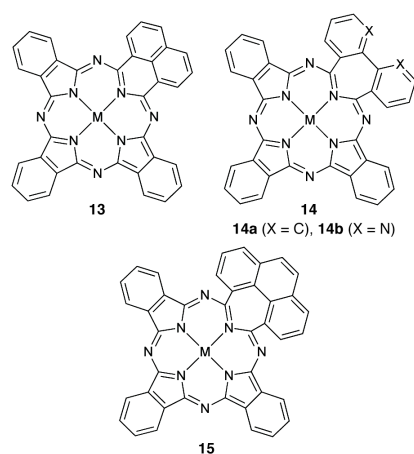
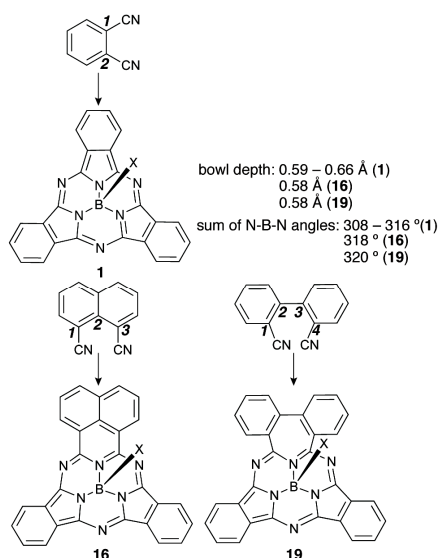


Fig. 9. Core-modified Pc analogues: a six-membered-ring-containing Pc analogue **13** and seven-membered-ring-containing Pc analogues **14** and **15**.

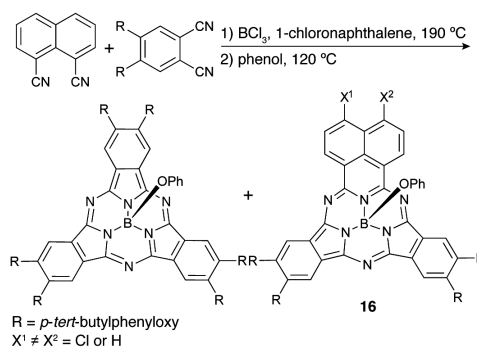


Scheme 3. Strategy towards core-modified SubPc analogues. The numeric characters written in the aromatic dicyanitrile precursors indicate the number of carbon atoms between cyano groups. Bowl-depth and sum of N-B-N angles are summarized.

3.1 Six-membered-ring-containing SubPc analogue

Six-membered-ring-containing SubPc analogue **16**, which is referred to as subazaphthalenephthalocyanine (SubAPPC), was obtained in an overall yield of 1.6% from a boron-templating reaction of 1,8-naphthalenedicarbonitrile and 4,5-di-*p*-tert-butylphenoxyphthalonitrile under similar conditions to those of conventional SubPcs, followed by axial ligand replacement from a chloride to a phenoxy group (Scheme 4).³⁵ Based on the mass spectrometric and NMR spectroscopic measurements, the structure of **16** with a chloro-substituent at the 4- or 5-position of the naphthalene moiety was anticipated. The X-ray single crystal analysis unambiguously revealed the chlorinated structure of **16** (Fig. 10). Despite optimization of the reaction conditions with the aim of obtaining a non-chlorinated species, only the chlorinated species was always formed probably due to

the high reactivity of **16** towards electrophilic aromatic substitution reaction.



Scheme 4. Synthesis of subazaphthalenephthalocyanine (SubAPPC **16**).

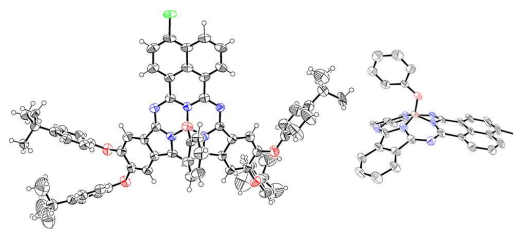


Fig. 10. X-ray single crystal structure of SubAPPC **16**, top view (left) and side view (right). The thermal ellipsoids were scaled to the 50% probability level. In the side view, *p*-tert-butylphenoxy substituents and hydrogen atoms were omitted for clarity (Reproduced from Ref. 35 with permission from Wiley).

In the crystal structure, **16** adopted a broadly similar bowl-shaped structure as is generally observed for SubPcs (Scheme 3). The bowl-depth of 0.58 Å defined by the distance of the central boron atom from the mean-plane of the three coordinating nitrogen atoms of the isoindole units (3N-plane) became only slightly shallower than that of SubPc (0.59–0.66 Å).¹ The strain caused by the incorporation of the six-membered-ring unit in the core was released by a planar arrangement of the azaphthalene moiety compared to the two isoindole units, which were tilted by about 23° from the mean plane of the three *meso*-nitrogen atoms. The position of the chloride atom could not be resolved due to disorder at the 4- and 5-positions with 7:3 occupancy, and the presence of the chloride-substituent generate an inherent chirality in **16** due to the absence of a mirror plane in the structure. In the molecular packing, both enantiomers were, therefore, observed.

16 exhibited complex and red-shifted Q band absorptions at 708, 659, 616, and 600 nm with respect to those of SubPcs at ca. 560–570 nm (Fig. 11).¹ Due to the variation of the main absorption in the visible region, the solution colour of **16** is blue rather than pink, which is a typical colour of SubPc. The fluorescence peak of **16** was observed at 718 nm with a Stokes shift of 197 cm⁻¹, and the fluorescence quantum yield and lifetime of 0.18 and 3.6 ns were comparable to those of SubPc.¹ The effect of the deformation of the structure from SubPc to **16** on the excited-state dynamics appears to be fairly insignificant.

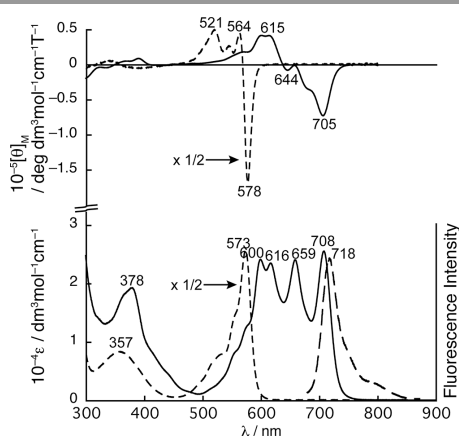


Fig. 11. UV/Vis absorption (bottom) and MCD (top) spectra of **16** (solid line) and SubPc with same substituents as a reference (dashed line) in CHCl_3 , and fluorescence spectrum of **16** (bottom, long dashed line) (Reproduced from Ref. 35 with permission from Wiley).

The MCD signals in the Q band region can be assigned as Faraday *B* terms, indicating non-degenerate excited states of **16**, which result from the absence of a threefold or higher molecular symmetry in the structure of **16** (Fig. 11).^{23–25} Since it is difficult to assign the split Q band absorptions from the MCD signal pattern, band deconvolution analysis was performed on the absorption and MCD spectra using band components with the same bandwidths and energies.³⁷ The complex Q band absorptions of **16** were tentatively assigned as overlapping pairs of Q_{00} and Q_{01} bands at 708 and 659 nm, respectively, followed by a more complex set of vibrational bands at higher energy.

The variation of the absorption spectral morphology and the electronic structure of **16** from SubPc is similar to that observed for asymmetric A_2B -type SubPc analogues with extra benzene rings at the periphery (**17** and **18**, Fig. 12).³⁸ A similar trend has also been demonstrated for the asymmetric A_3B -type Pc analogues, the details of which were described elsewhere.³⁹ In the following section, the electronic structure of **16** is described by comparison with that of seven-membered-ring-containing SubPc analogues.

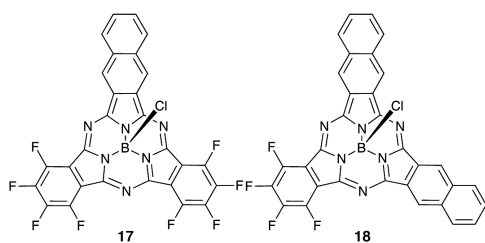
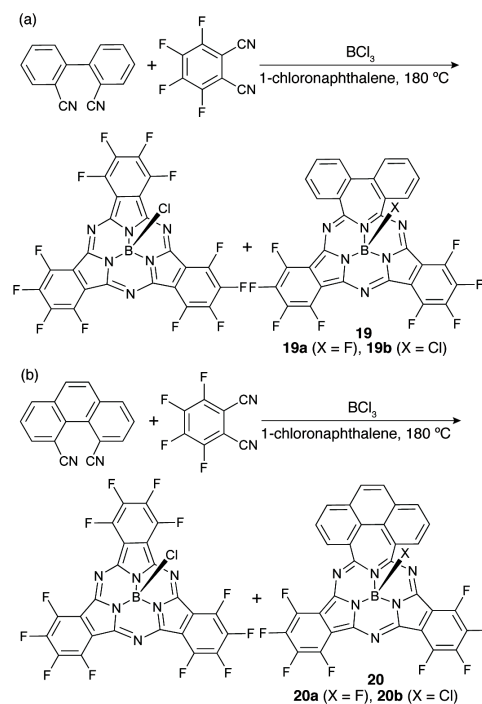


Fig. 12. Representative A_2B - and AB_2 -type SubPcs **17** and **18**.

3.2 Seven-membered-ring-containing SubPc analogue

The above-mentioned core-modification strategy was further expanded to synthesize seven-membered-ring-containing SubPc analogues (**19** and **20**, Scheme 5).³⁶ To generate a seven-membered-ring unit in the core, 2,2'-biphenyldicarbonitrile and 4,5-phenanthrenedicarbonitrile, which contains cyano groups at positions with a 1,4-

relationship, were selected. Under similar SubPc synthetic conditions using a mixture of these phthalonitrile derivatives and tetrafluorophthalonitrile in the presence of boron trichloride, seven-membered-ring-containing SubPc analogues, **19a** and **20a**, were formed in 9.1 and 9.8% yield, respectively. Although molecular ion peaks corresponding to structures with an axial chloride ligand (**19b** and **20b**) were observed, more intense signals of the axially fluorinated species were, to our surprise, detected as major ion peaks. The presence of the axial fluorine ligand in **19a** and **20a** was confirmed by ^{11}B and ^{19}F NMR spectra, which exhibited the fluorine signals as a quartet at -149.6 ppm for **19a** and at -149.4 ppm for **20a** and the boron signals as a doublet at -11.7 ppm for **19a** and at -11.5 ppm for **20a**. These boron and fluorine signal patterns are characteristic of the B–F coupling. A control experiment using *o*-phthalonitrile instead of tetrafluorophthalonitrile provided neither **19a** and **20a** nor **19b** and **20b**. This result led us to assign the origin of the axial fluorine atom to decomposition of tetrafluorophthalonitrile during the reaction.



Scheme 5. Synthesis of seven-membered-ring-containing SubPc analogues, (a) **19** and (b) **20**.

The structure of **19a** broadly adopted a similar bowl-shaped structure to that of SubPc¹ and SubAPPC **16**,³⁵ whereas the dihedral angle of the biphenyl moiety from the 3N-plane by 43° was markedly different as compared to the planar arrangement of the azaphenylene unit in **16** (Fig. 13). This is due to the incorporation of the large seven-membered-ring unit in the core. In the case of the seven-membered-ring-containing Pc analogues **14** and **15** (Fig. 9), a similar significant tilt of the biphenyl moiety was also observed.^{34b,c} This large tilt of the biphenyl moiety caused helicity of the seven-membered-ring unit, which enabled **19a** to exist as *P* and *M* enantiomers. In the

molecular packing diagram, these enantiomers stacked alternately to form one-dimensional columnar packing as a result of the π - π interactions, which was enhanced by the small fluorine axial ligand.⁴⁰

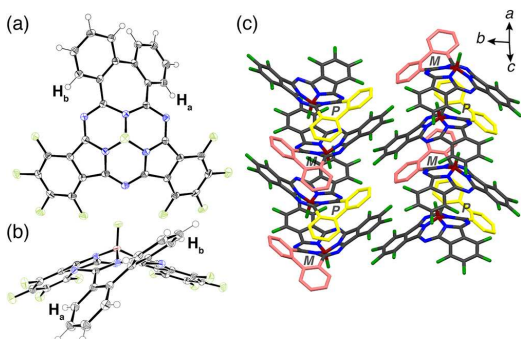


Fig. 13. X-ray single crystal structure of **19a**, (a) top view, (b) side view, and (c) packing diagram. The thermal ellipsoids were scaled to the 50% probability level. In the packing diagram, the biphenyl units of the *P* and *M* enantiomers are highlighted (Reproduced from Ref. 36 with permission from Wiley).

A plausible reason for the formation of **19a** instead of **19b**, which is considered as a conventional product, could lie in the slight variation of the structural features of **19** compared to those of SubPc¹ and **16**³⁵ (Scheme 3). A more planar coordination geometry of the central boron atom in **19** was implied by the shallower bowl depth of 0.57 Å defined by the deviation of the central boron atom from the 3N-plane with respect to that observed for SubPc (0.59–0.66 Å) and **16** (0.58 Å). The sum of the N-B-N angles also increased in this order (SubPc: 308–316°, **16**: 317.5°, and **19a**: 319.9°). This slightly planarized coordination geometry around the central boron atom resulted in the preferential formation of the axially fluoro-substituted **19a** and **20a** over the axially chloro-substituted **19b** and **20b**.

The incorporation of the seven-membered-ring unit further led to dynamic molecular motion between the *P* and *M* enantiomers in solution, which was demonstrated by variable temperature ¹H NMR measurements. Despite the absence of any symmetry element in the structures of **19a** and **20a**, the ¹H NMR spectra of these compounds at room temperature showed symmetric peak patterns due to the biphenyl and phenanthrene moieties (**19a**: 8.04, 7.74, 7.68, and 7.59 ppm, **20a**: 8.60, 8.15, 7.92, and 7.87 ppm). Upon lowering the temperature, these proton signals of **19a** became broad and then coalescent at –40 °C, and six peaks at 8.07, 7.78, 7.73, 7.70, 7.64, and 7.46 ppm appeared at –80 °C, whereas only a slight upfield shift of the single proton signal of hydrogen atoms at the 3- and 6-positions of the phenanthrene moiety was observed for **20a**. These results indicated that the fluttering dynamic motion of **19a** was thermally suppressed with an activation energy of 10.7 kcal mol⁻¹ at –40 °C,⁴¹ while that of **20a** was still maintained because of the smaller activation energy caused by the fused structure of the phenanthrene moiety. The assignment of the proton signals of **19a** at –80 °C based on the H,H COSY experiment and DFT calculations at the B3LYP/6-311G(2d,p) level revealed an explicit difference in the chemical shift of the

biphenyl hydrogen atoms above and below the molecule, particularly for H_a and H_b at 8.07 and 7.78 ppm, respectively (Fig. 13). Taking a similar distance of these hydrogen atoms either from the centre or the rim into consideration, the downfield shift of H_a can be ascribed to a larger deshielding diatropic ring-current effect originating from the concave surface relative to the convex surface. As Torres and co-workers have recently reported, in order to study the difference in ring-current effect and electronic interactions between the convex and concave surfaces,^{42,43} SubPc and its analogues can be a useful probe to investigate their electronic structures, which has placed it in the centre of research interests in the field of conjugated molecules bearing the curved surfaces, as exemplified by nanocarbons, such as fragmentary structures of fullerene and carbon nanotube.⁴⁴

Compared with the single Q band absorption of SubPc at ca. 560 nm,¹ both **19a** and **20a** showed markedly split Q band absorptions in the shorter and longer wavelength regions at 510 and 682 nm and 513 and 693 nm, respectively (Fig. 14). The fluorescence peaks of **19a** and **20a** were observed at 710 and 706 nm with fluorescence quantum yields of 0.08 and 0.006, respectively. The smaller quantum yield of **20a** also evidenced its more flexible structure, as indicated by the above-mentioned variable temperature ¹H NMR measurements. In the MCD spectra, both compounds showed Faraday *B* terms corresponding to the split Q band absorptions, which were indicative of the presence of non-degenerate excited states.^{23–25} These absorption and MCD spectral features appeared to be characteristic of tetraazachlorin-type Pc analogues,^{39e,45} in which part of the peripheral double bond is reduced to sp³-hybridized carbon atoms. Hence, this implied changes in the electronic structure of SubPc by incorporation of the seven-membered-ring unit, the details of which are discussed in the following section.

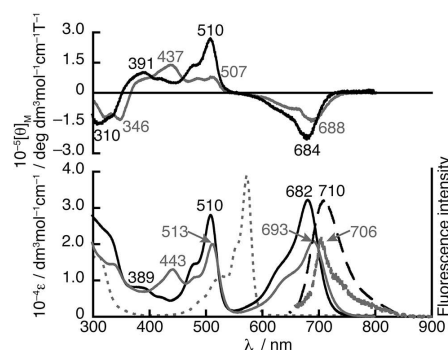


Fig. 14. UV/Vis absorption (bottom, solid lines), MCD (top), and fluorescence spectra (bottom, dashed lines) of **19a** (black) and **20a** (gray) in CHCl₃. The normalized UV/Vis absorption spectrum of SubPc with same substituents in CHCl₃ is shown as a reference (the intensity is shown in arbitrary units; bottom, gray dotted line) (Reproduced from Ref. 36 with permission from Wiley).

3.3 Comparison of the electronic structures of SubPc and core-expanded SubPc analogues

Since the frontier molecular orbitals of SubPc and its analogues directly relate to the absorption spectral

morphologies in the Q band region,^{22–24} comparison of the MO energy diagrams of the core-modified SubPc analogues, **16**, **19**, and **20** with those of SubPc with similar axial ligands and peripheral substituents was performed in order to reveal the trends associated with the changes in the electronic structures of these compounds.

16 showed similar density distribution patterns of the frontier MOs to SubPc, and the MO coefficients were also found on the naphthalene moiety (Fig. 15).³⁵ Comparing its energy levels with those of SubPc, the HOMO was significantly destabilized, whereas a similar energy of the LUMO was predicted. The LUMO and LUMO+1 became non-degenerate in the case of **16** with an energy difference of 0.08 eV, which was caused by the lowering the molecular symmetry by ring-expansion from the five-membered pyrrole ring to the six-membered azaphenylene ring. The TDDFT calculations on this basis well reproduced the observed absorption spectrum of **16**. Cyclic voltammetry measurements demonstrated a negative-shift of the oxidation potential and a similar reduction potential with respect to those of SubPc as a reference compound, which reflected the highly-lying HOMO and similar energy LUMO.

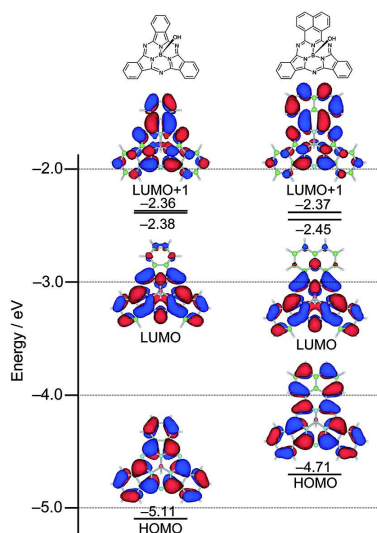


Fig. 15. Partial frontier MO diagrams of **16** (right) and reference SubPc (left). The model structures used for the calculation are shown above (Reproduced from Ref. 35 with permission from Wiley).

The density distribution patterns of the frontier MOs of **19a** and **20a** were basically similar to those of SubPc, indicating that they retained 14π -electron conjugated systems as a SubPc analogue (Fig. 16).³⁶ Delocalization of these MOs on the seven-membered azepine ring implied that it contributed to the conjugated systems of **19a** and **20a** to some degree. Similarly to **16**, significant destabilization of the HOMO was predicted. In addition, non-degeneracy of the LUMO and LUMO+1 became more pronounced in the cases of **19a** and **20a**. Despite the delocalization of the MOs over the entire molecular structure, their MO energy diagram appeared to be similar to those of chlorin-type compounds. This could be explained by considering the significant large twist of the seven-membered-ring unit as observed in the crystal structure of **19a**. The

theoretical absorption spectra predicted by the TDDFT calculations on this basis were in good agreement with the observed absorption spectra. Furthermore, the TDDFT calculations assigned the origin of the red-shifted absorption of **20a** at 443 nm with respect to that of **19a** at 389 nm, to destabilization of the HOMO–1, which is localized on the outer biphenyl or phenanthrene moieties.

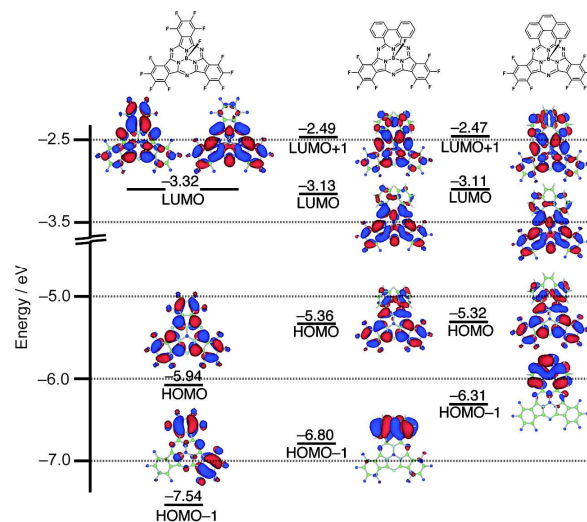


Fig. 16. Partial frontier MO diagrams of reference SubPc (left), **19a** (middle), and **20a** (right). The model structures used for the calculation are shown above (Reproduced from Ref. 36 with permission from Wiley).

In summary, in the comparison of the electronic structures between SubPc, **16**, **19**, and **20**, incorporation of the six-membered-ring unit caused destabilization of the HOMO and a slight non-degeneracy of the LUMO and LUMO+1, whereas incorporation of the seven-membered-ring unit led to destabilization of the HOMO and LUMO+1. As these variations of the MO diagrams were similarly observed for the periphery β,β -benzo-annulated Pc analogues³⁹ and tetraazachlorin analogues,^{39e,45} respectively, the effect of core-modification can be regarded as well.

4. Exterior-modification

Exterior-modification (Fig. 3), removal of the peripheral benzo moieties or replacement of these with other fused ring units, is generally more feasible compared to the above-mentioned modification of the bridging unit and core-modification, as long as precursory *o*-phthalonitrile derivatives with enough reactivity are available. Representative examples of exterior-modified SubPc analogues are 2,3-subnaphthalocyanine **21**⁴⁶ and subtriazaporphyrin (subporphyrazine **22**),⁴⁷ in which extra benzene rings are fused to SubPc and the peripheral benzene rings are removed from SubPc, respectively (Fig. 17). As another unique family member, a benzo-annulated SubPc dimer **23**⁴⁸ and trimer **24**⁴⁹ have also been reported. As described above, these compounds are available due to the existence of the corresponding dinitrile precursors, 2,3-naphthalenedicarbonitrile, fumaronitrile, and

1,2,4,5-tetracyanobenzene and their sufficient reactivities in the SubPc syntheses. This in turn may indicate that once dinitrile precursors with fused aromatic ring units or functional units are in hand, there is a chance to synthesize the corresponding SubPc analogues with these units at the periphery, which can endow novel properties to SubPc. According to this synthetic strategy, novel exterior-modified SubPc analogues have been synthesized, and either novel properties, such as chlorin-like optical properties and multiple redox behaviours, or enhancement of the inherent properties of SubPc, such as convex-concave interactions and molecular chirality, have been achieved.

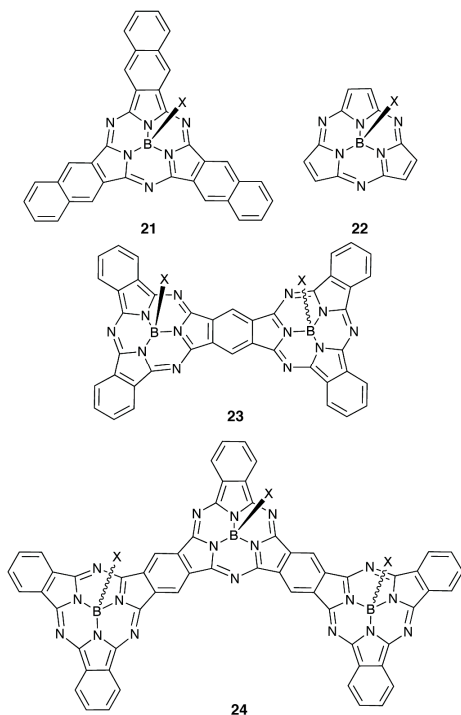


Fig. 17. 2,3-Subnaphthalocyanine **21**, subtriazaporphyrin **22**, SubPc dimer **23**, and SubPc trimer **24**.

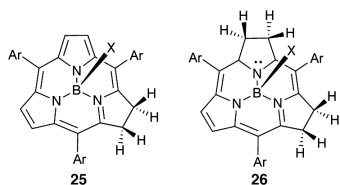


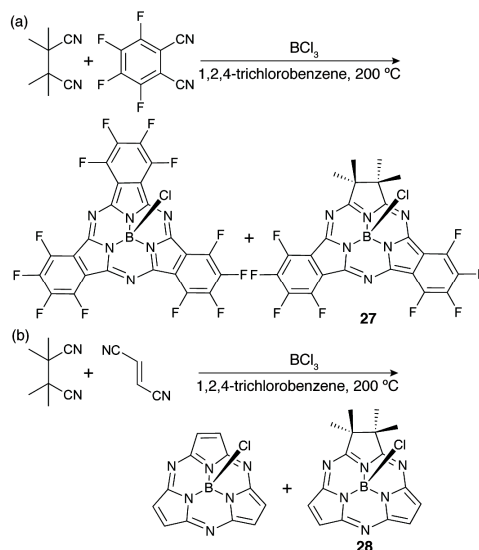
Fig. 18. meso-Aryl-substituted subchlorin **25** and subbacteriochlorin **26**.

4.1 β,β -sp³-Hybridized subphthalocyanine analogues

Chlorin, which comprises a β,β -hydrogenated structure of porphyrin, is a naturally occurring porphyrinoid.⁵⁰ Because of its importance in the light harvesting antenna and energy- and electron-transfer processes in photosynthesis, porphyrin and Pc analogues with chlorin-like conjugated systems have been intensively pursued in order to achieve their superior and more

intense Q band absorption compared to regular porphyrins and Pcs.^{45,51} In the chemistry of sub-species, a chlorin-type molecule was only recently synthesized by Osuka *et al.* as a major byproduct in the synthesis of meso-aryl-substituted subporphyrins (**25**, Fig. 18).⁵² They successively reported a bacteriochlorin-type subporphyrin analogue **26**, in which the β,β -positions of two pyrrole rings were sp³-hybridized.⁵³ Despite the importance of a chlorin-type SubPc analogue, it has been a kind of missing link in the family of porphyrin and Pc analogues. In the course of our investigation on exterior-modified SubPc analogues along with the above-mentioned synthetic strategy, we noticed the utility of tetramethylsuccinonitrile, which was a synthetic precursor of tetraazachlorin in our previous works,^{39e,45} in the synthesis of novel chlorin-type SubPc analogues, dibenzosubtriazachlorin (DBSubTAC **27**) and subtriazachlorin (SubTAC **28**).⁵⁴

DBSubTAC **27** was synthesized from a mixed-condensation reaction of tetramethylsuccinonitrile and tetrafluorophthalonitrile in 1.2% isolated yield (Scheme 6).⁵⁴ Similarly its benzene-ring-abstracted analogue **28** was synthesized using fumaronitrile instead of tetrafluorophthalonitrile, but the yield was significantly low (0.1%) due to the low reactivity of fumaronitrile.



Scheme 6. Synthesis of subtriazachlorin analogues, (a) DBSubTAC **27** and (b) SubTAC **28**.

Two characteristic singlet proton signals at 2.03 and 1.16 ppm for **27** and 1.13 and 1.09 ppm for **28** in the ¹H NMR spectra evidenced the incorporation of a β,β -sp³-hybridized pyrrole into the structures. The difference of these chemical shifts was ascribed to the presence of the methyl substituents above and below the molecule and consequent difference in the ring current effect. The structure of **27** was unambiguously elucidated by single crystal X-ray analysis (Fig. 19). The structural feature of **27** was broadly similar to those of SubPc,¹ such as a bowl-depth of 0.58 Å defined as the distance from the boron atom to the 3N-plane. The bond length of the sp³-

hybridized C-C bond was in the range of a single bond distance (1.602(3) Å).

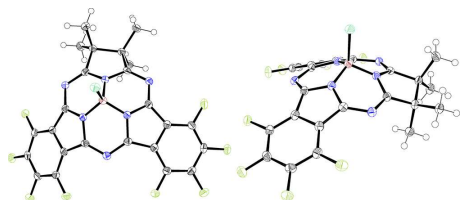


Fig. 19. X-ray single crystal structure of **27**, top view (left) and side view (right). The thermal ellipsoids were scaled to the 50% probability level (Reproduced from Ref. 54 with permission from The Royal Society of Chemistry).

As is commonly observed for the absorption spectra of chlorin-type porphyrin⁵¹ and Pc analogues,⁴⁵ both **27** and **28** exhibited markedly split Q band absorptions, which included a sharp band at 632 nm for **27** and at 561 nm for **28** and a rather broad, weak band at 454 nm for **27** and at 383 nm for **28**, in the longer and shorter wavelength regions with respect to the single Q band absorption of SubPc (Fig. 20). Corresponding to these split Q band absorptions, negative-to-positive Faraday *B* terms were observed in the MCD spectra, which enabled assignment of these split absorptions as Q bands despite the significant difference in their relative intensities.²³⁻²⁵ According to our previous works on tetrazachlorin compounds, the low intensities of the higher-energy Q band absorptions can be ascribed to configuration interaction with the Soret band with an incidentally close energy.^{45d} The Q band spectral features of **27** and **28** can, therefore, be explained as well. Both **27** and **28** also exhibited mirror-imaged fluorescence with respect to the lower-energy Q band absorption.

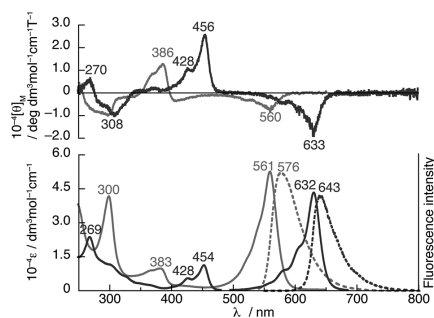


Fig. 20. UV/Vis absorption (bottom, solid lines), fluorescence (bottom, dotted lines), and MCD (top) spectra of **27** (black) in CHCl₃ and **28** (gray) in CH₂Cl₂ (Reproduced from Ref. 54 with permission from The Royal Society of Chemistry).

As a result of the loss of conjugation at the sp³-hybridized β,β-positions, the HOMO and LUMO+1 become destabilized in the MO diagrams of **27** (Fig. 21) and **28** as compared to those of the reference SubPc and subtriazaporphyrin. The destabilization of the LUMO+1 caused non-degeneracy of the LUMO and LUMO+1. Since the Q band absorptions mainly comprise transitions from the HOMO to the LUMO and LUMO+1 based on the TDDFT calculations, the variation of the electronic structures of these chlorin-type SubPc analogues were in good agreement with the observed split nature of the Q band absorptions. The negative shift of the first oxidation

potential as well as the small potential change in the first reduction observed in the cyclic voltammetry measurement of **27** relative to those of SubPc also supported the trend in the MO energy diagram. It can, therefore, be concluded that the electronic structures of **27** and **28** possess a chlorin-like conjugated system as anticipated from their structures.

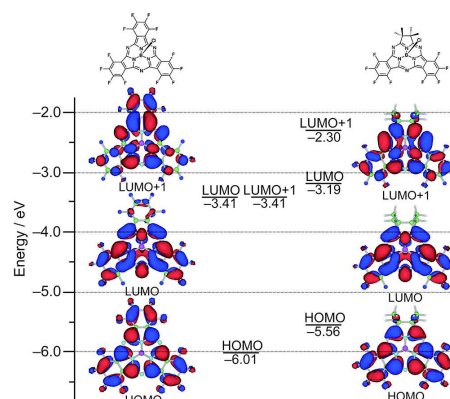
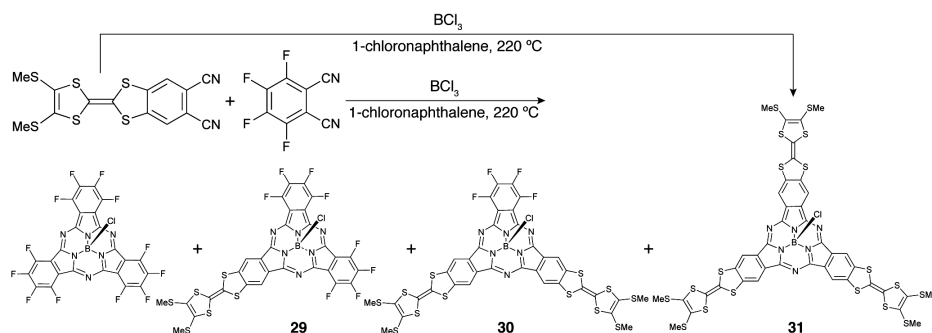


Fig. 21. Partial frontier MO diagrams of **27** (right) and reference SubPc (left). The model structures used for the calculation are shown above (Reproduced from Ref. 54 with permission from The Royal Society of Chemistry).

4.2 Tetrathiafulvalene-annulated SubPc

In addition to complex functionality of exterior-modified SubPc, annulation of functional units onto the periphery of SubPc also enables the symmetric arrangement of those functional units with an angle of 120°. As a choice of functional units, tetrathiafulvalene (TTF)⁵⁵ is of interest as a variety of TTF-annulated porphyrins and Pcs have been elaborated with the expectation to create complex functionality.^{56,57} However one of the main drawbacks in the TTF-annulated Pc systems is their inherent poor solubility due to their completely planar structures and strong tendency towards π-π stacking of both the Pc and TTF units. This often hinders complete characterization and analysis of their optical and electrochemical properties. In addition to the C₃-symmetric arrangement of TTF units, the solubility problem should be improved in the case of the TTF-annulated SubPc system, so that properties stemming from the annulation of TTF units to SubPc could, therefore, be unambiguously disclosed.⁵⁸

A series of TTF-annulated SubPcs **29-31** were synthesized from a mixed-condensation reaction of TTF-annulated *o*-phthalonitrile and tetrafluorophthalonitrile in rather poor yield (**29**: 0.5%, **30**: 0.6%, **31**: trace, Scheme 7).⁵⁸ Self-condensation reaction of TTF-annulated *o*-phthalonitrile provided only tri-TTF-annulated SubPc **31** in much improved yield (2%). The number of TTF units incorporated in these compounds and the arrangement of the TTF units in C_s-symmetry for **29** and **30** and C_{3v}-symmetry for **31** was confirmed based on mass spectrometry and ¹H NMR spectroscopy. Methylthio protons were observed as a singlet at 2.47 ppm for **29**, a pair of singlets at 2.46 ppm for **30**, and a singlet at 2.47 ppm for **31**, whereas the α-benzo protons appeared in the aromatic region at 8.69 ppm for **29**, 8.59 and 8.66 ppm for **30**, and 8.47 ppm for **31**.



Scheme 7. Synthesis of TTF-annulated SubPc analogues **29**–**31**.

The absorption spectra of these TTF-annulated SubPcs exhibited red-shift and broadening of the Q band absorptions upon increasing the number of fused TTF units (**29**: 578 nm, **30**: 584 nm, **31**: 593 nm), while the Soret band region in the far-violet and UV regions varied dramatically due to the presence of the Soret band of SubPc and the absorption of the TTF units (Fig. 22). Compared to the split Q band absorptions observed for the low symmetry A_2B and AB_2 -type benzene-fused SubPcs **17** and **18** (Fig. 12),³⁸ the single Q band absorptions of **29** and **30** were indicative of a fairly small perturbation by the TTF units to the excited states of the SubPc core. As described in the previous section, MCD spectroscopy on SubPc analogues provides information about the relative energy difference between the LUMO and LUMO+1.^{23–25} A Faraday A term corresponding to the Q band absorption of all the TTF-annulated SubPcs implied degeneracy of their excited states (Fig. 22). In light of the low molecular symmetries, the Faraday A terms of **29** and **30** were actually closely-lying Faraday B terms. These Faraday B terms are referred to as a pseudo Faraday A term, which is commonly observed when molecules possess non-degenerate excited states with accidentally small energy differences.^{24a,59}

The fluorescence spectra of **29**–**31** exhibited gradual quenching of their fluorescence upon increment of the number of fused-TTF units (Fig. 22). The fluorescence quantum yields decreased from **29** ($\Phi_F = 0.06$) to **30** ($\Phi_F = 6.1 \times 10^{-4}$), and no fluorescence was observed for **31**. This fluorescence quenching can be explained in terms of electron-transfer from TTF moieties to SubPc in the excited states, which can be generally observed for TTF-annulated porphyrins and Pcs.^{56,57}

Cyclic voltammetry measurements on these SubPc analogues provided further information about the frontier MOs and their relative energies (Fig. 23). Considering the similar oxidation potentials observed for TTF-annulated *o*-phthalonitrile, and the increase in the number of electrons involved in each oxidation process from one-electron for **29** to two-electron for **30** and further to three-electron for **31**, the oxidation processes of the TTF-annulated SubPcs appeared to be centred on the TTF moieties. In addition, the small variation in the oxidation potentials also inferred negligible interaction between each TTF moiety. Spectroelectrochemistry by applying potentials more anodic than the first oxidation as well as absorption spectrum measurements upon chemical oxidation demonstrated appearance of a broad absorption centred at ca.

800 nm due to the generation of the TTF radical cations (Fig. 24). Intensification of the Q band absorption upon further oxidation indicated a rather significant contribution of transitions from the TTF-centred orbitals to the Q band absorption.

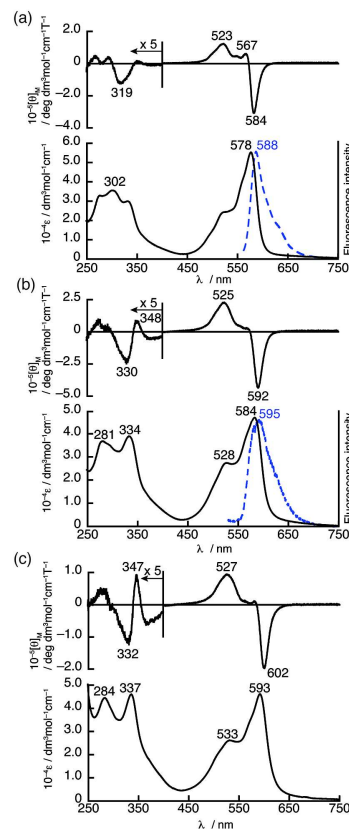


Fig. 22. UV/Vis absorption (bottom, solid line), fluorescence (bottom, dashed line), and MCD (top) spectra of (a) **29**, (b) **30**, and (c) **31** in CHCl_3 (Reproduced from Ref. 58 with permission from Wiley).

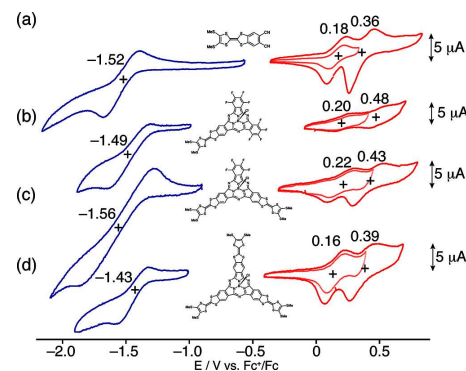


Fig. 23. Cyclic voltammograms of (a) TTF-annulated *o*-phthalonitrile, (b) **29**, (c) **30**, (d) **31** (0.5 mM) in *o*-dichlorobenzene containing 0.1 M tetrabutylammonium perchlorate as a supporting electrolyte at a scan rate of 100 mV s^{-1} . Values are half-wave potentials (Reproduced from Ref. 58 with permission from Wiley).

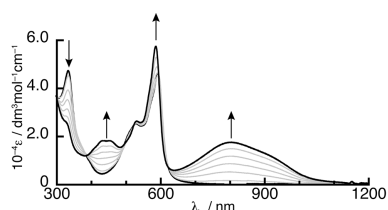


Fig. 24. UV/Vis spectral changes upon chemical oxidation of **31** with $\text{Fe}(\text{ClO}_4)_3 \cdot n\text{H}_2\text{O}$ in a mixture of CHCl_3 and CH_3CN (v/v 2:1) (Adapted from Ref. 58 with permission from Wiley).

MO diagrams of these TTF-annulated SubPcs based on DFT calculations at the B3LYP/LANL2DZ level revealed non-degeneracy and degeneracy of the LUMOs for **29** and **30** and for **31**, respectively, and a slight destabilization of their energy levels upon increasing the number of the TTF units (Fig. 25). In contrast, the HOMOs (HOMO of **29**, HOMO and HOMO–1 of **30** and HOMO, HOMO–1, and HOMO–2 of **31**) were localized on the TTF moieties, while the following occupied orbitals were centred on the SubPc core, the energy levels of which were significantly destabilized in the order from **29** to **30** and to **31**. TDDFT calculations revealed that the Q band absorptions mainly comprise transitions from the SubPc-centred occupied orbital (HOMO–1 for **29**, HOMO–2 for **30**, and HOMO–3 for **31**) to the LUMO and LUMO+1. The broad nature of the Q band absorptions was also ascribed to the presence of transitions from the TTF-centred HOMOs to the LUMO and LUMO+1. These calculation results reproduced the observed absorption spectral features of the TTF-annulated SubPcs and their TTF-centred oxidation processes.

As a whole, this investigation showed that SubPc can be utilized as a scaffold for arranging functional units in a symmetric manner with rather insignificant interactions between those units. Complex functionality such as TTF-centred oxidation processes and broadening of the Q band absorption due to the interaction with the TTF moieties and the SubPc core was also achieved.

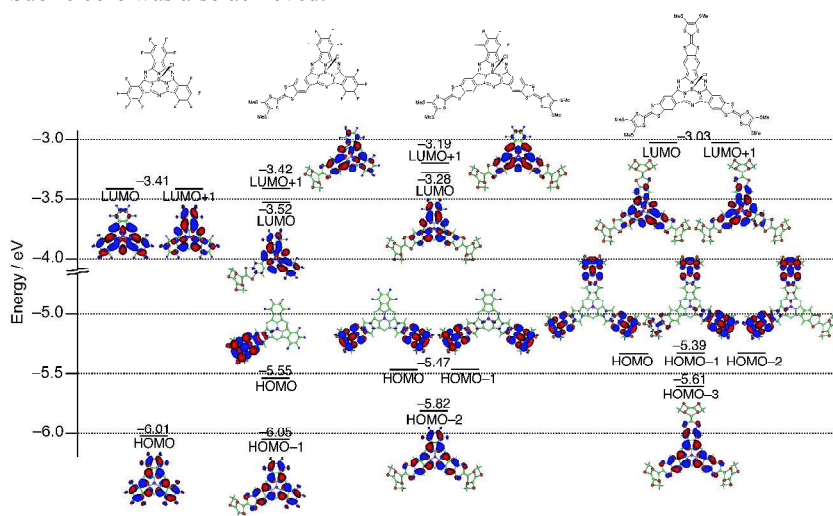


Fig. 25. Partial frontier MO diagrams of TTF-annulated SubPc and reference SubPc (left). The model structures used for the calculation are shown above (Reproduced from Ref. 58 with permission from Wiley).

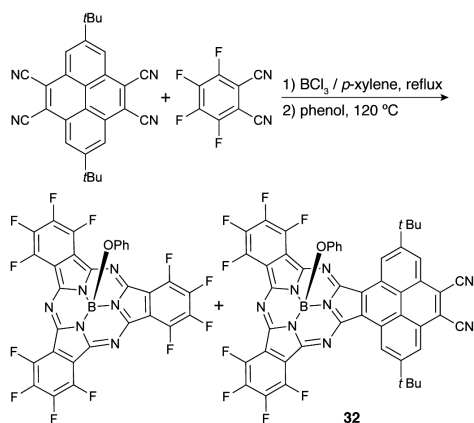
4.3 Pyrene-fused SubPc

Following the recognition of fullerenes and carbon nanotubes as key materials in the nanotechnology, conjugated molecules with curved π -conjugated surfaces, which can provide convex-concave supramolecular interactions with those nano carbon materials due to high structural affinities, have become an important class of functional molecules.^{44,60-62} In this respect, SubPc appears to be a highly potential candidate. Torres and Claessens pioneered this research direction and demonstrated facile encapsulation of a C_{60} molecule into a cage-like SubPc dimer.⁶³ Although a convex-concave interaction between SubPc monomer and C_{60} molecules in solution was recently proposed based on an absorption spectral titration study and transient absorption spectroscopy by the same group,⁶⁴ there has been no report on this type of supramolecular complex in the solid state. As co-crystallization of genuine SubPc and fullerenes has been unsuccessful probably due to small supramolecular interactions, exterior-modification of SubPc with a pyrene moiety was, then, designed with an aim to enhance donor ability.⁶⁵

A mixed-condensation reaction of a key precursory nitrile, 2,7-di-*tert*-butyl-4,5,9,10-tetracyanopyrene, and tetrafluorophthalonitrile provided **32** in 8.3% yield (Scheme 8), which was much improved from our previous report (0.9% yield).^{65,66} The structure of **32** was determined by mass spectrometry and NMR spectroscopy as well as X-ray single-crystal crystallography (Fig. 26). As a result of the deshielding ring current effect, one proton signal of the pyrene moiety at 10.71 ppm shifted downfield with respect to the other at 8.85 ppm. The crystal structure of **32** exhibited very similar structural features to those of regular SubPc¹ except for the presence of the fused pyrene moiety. In the molecular packing diagram, **32** formed π - π stacking of the pyrene moieties in a concave-concave fashion with the next neighbour and π - π stacking between the axial phenyl ligand and the pyrene moiety in a convex-convex fashion with the other next neighbour.

The mutual packing diagram observed for **32** due to the strong π - π stacking ability of the pyrene moiety enabled the first co-crystallization with a C_{60} molecule. Slow diffusion of hexane into a toluene solution of a 2:1 mixture of **32** and C_{60} provided black, brick-like co-crystals. The severe disorder of C_{60} molecules in the structure, which is often a feature in fullerene-containing crystal structures, made it difficult to determine the exact positions of the carbon atoms of C_{60} molecules,⁶⁷ but the structural features could be suitably deduced (Fig. 27). Two **32** molecules embraced a C_{60} molecule, and both the pyrene moiety and the concave surface of the SubPc moiety formed π - π stacking with a C_{60} molecule with an intermolecular separation of *ca.* 3.3 Å. The opposite surface of the pyrene moiety had π - π stacking with the axial phenoxy ligand of the nearest neighbour to form a

supramolecular dimer in a convex-convex fashion. This molecular packing diagram, therefore, led to a one-dimensional zigzag array of **32**, in which C_{60} molecules were linearly ordered along the a -axis and b -axis with centre-to-centre separations of the C_{60} molecules of 16.9 Å and 14.8 Å, respectively.



Scheme 8. Synthesis of pyrene-fused SubPc **32**.

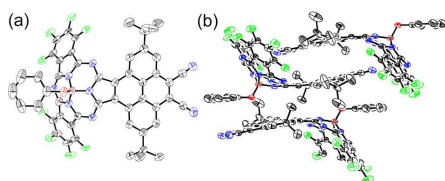


Fig. 26. X-ray single crystal structure of **32**, (a) top view and (b) molecular packing diagram. The thermal ellipsoids were scaled to the 50% probability level. Hydrogen atoms were omitted for clarity (Reproduced from Ref. 65 with permission from The Royal Society of Chemistry).

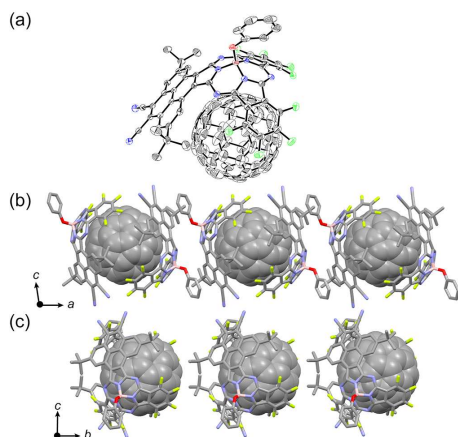


Fig. 27. X-ray single crystal structure of cocrystallate of **32** and C_{60} , (a) top view and (b and c) molecular packing diagrams. The thermal ellipsoids were scaled to the 50% probability level. Hydrogen atoms were omitted for clarity (Reproduced from Ref. 65 with permission from The Royal Society of Chemistry).

The high affinity of **32** to C_{60} encouraged us to investigate the possibility of supramolecular interaction in solution. The absorption spectrum of the dissolved co-crystals in $CHCl_3$, however, merely showed a summation of the absorption spectra of **32** and C_{60} , indicating an absence of supramolecular interactions in solution. Although supramolecular interaction in

solution has not yet been achieved in this system, the unique chemistry of **32** allowed us to tentatively conclude that exterior-modification with π -donor units is an important concept of the molecular design towards molecular recognition in solution and supramolecular architecture in the solid state.

4. 4,1,2-Subnaphthalocyanines and their chiroptical properties

As a synthesis of SubPc from *o*-phthalonitrile derivatives with asymmetric substitution lowers the C_{3v} -symmetry of SubPc to C_3 - or C_1 -symmetries with respect to the arrangement of the substituents, the absence of a mirror plane in the resultant SubPc structures causes an inherent molecular chirality. This possibility was demonstrated for the first time by Torres and Calessens with tri- β -iodo-substituted SubPc synthesized from asymmetric 4-iodophthalonitrile, and they succeeded in separating the C_3 - and C_1 -symmetric diastereomers (**33** and **34**, Fig. 28).⁶⁸ In 2002, our group achieved the first separation of enantiomers of C_3 -symmetric SubPc **35** with nitro and *tert*-butyl substituents at the α - and β -positions, respectively.⁶⁹

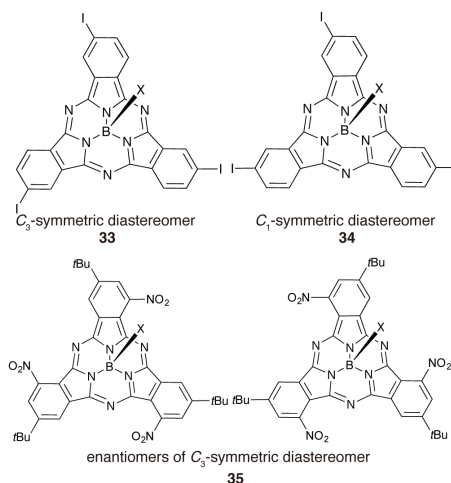
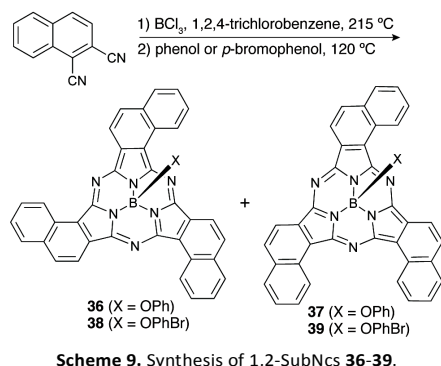


Fig. 28. C_3 - and C_1 -symmetric diastereomers **33** and **34**, and enantiomers of a C_3 -symmetric diastereomer **35**.

Despite these pioneering works, complete separation and characterization of all the diastereomers and enantiomers of chiral SubPc analogues has been hampered mainly by the small structural differences of the diastereomers and the low solubilities of the previously reported chiral SubPcs. For further study of the structure-chirality relationship, SubPc molecules with moderate solubility in common organic solvents and with small variations in the optical properties were required. Considering that annulation of benzene rings to the α , β -peripheral positions of Pc does not affect the absorption spectral features,⁷⁰ we chose the exterior-modified SubPcs with benzo-annulation at the α , β -peripheral positions as a key structure for the study of the chiral SubPc with an aim to improve solubility and structural differences between C_3 - and C_1 -symmetric diastereomers.⁷¹

A conventional SubPc synthetic reaction of 1,2-naphthalenedicarbonitrile using boron trichloride as a template, followed by an *in situ* axial ligand exchange from chloride to

phenoxy using phenol provided the target 1,2-subnaphthalocyanines (1,2-SubNcs, Scheme 9).⁷¹ C_3 and C_1 diastereomers of 1,2-SubNcs (**36** and **37**) were, then, successfully separated by silica gel column chromatography in 1.6% and 5.7% yields, respectively. These yields were not poor because approximately 70% of the starting 1,2-naphthalenedicarbonitrile was recovered. In order to determine the absolute structures of these compounds by X-ray crystallographic analysis based on the Bijvoet method,⁷² axially *para*-bromophenyl-substituted species (**38** and **39**) were also synthesized and purified by following the same procedure.



The ¹H NMR spectra of the C_3 -symmetric diastereomers (**36** and **38**) exhibited six proton signals due to the naphthalene moieties in the aromatic region, whereas the C_1 -symmetric diastereomers (**37** and **39**) showed two sets of six proton signals at similar chemical shifts to those of the C_3 -symmetric diastereomers. These ¹H NMR signal patterns were in good agreement with their molecular symmetries, which was further elucidated by the X-ray crystallographic analysis (Fig. 29).

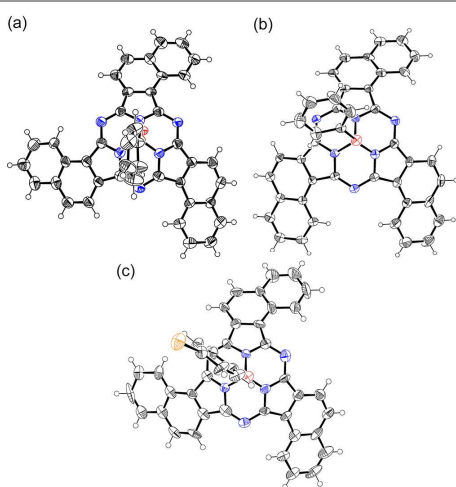


Fig. 29. X-ray single crystal structures of (a) **36**, (b) **37**, and (c) **38Fr1** (a structure of one of the enantiomers is shown for **36** and **37**). The thermal ellipsoids were scaled to the 50% probability level (Reproduced from Ref. 71 with permission from ACS).

The electronic absorption spectra of **36** and **37** have essentially similar shapes to that of SubPc,¹ including values of the molar absorption coefficient as well as positions of the Q

band absorption at 575 nm (Fig. 30 and 31). The only slight red-shift by only 10 nm from that of unsubstituted SubPc implied small perturbation of the benzo-annulation at the α,β -positions to the electronic structure of SubPc, as was initially anticipated. In contrast, the Soret band region from 250 to 450 nm varied quite significantly with the appearance of three bands at 388, 346, and 291 nm for **36** and at 390, 342, and 290 nm for **37**. Similar spectral morphologies between **36** and **37** were also observed in the MCD spectra, exhibiting a Faraday A term for the Q band absorption of **36** and a pseudo Faraday A term for that of **37**,^{24a,59} and dispersion type MCD signals for both geometric isomers in the Soret band region. The slight variation of the Q band region and rather significant changes in the spectral morphology in the Soret band region can be explained based on DFT and TDDFT calculations, which demonstrated maintenance of the energy levels and degeneracy of the LUMO and LUMO+1 and destabilization of the HOMO-3 (Fig. 32).

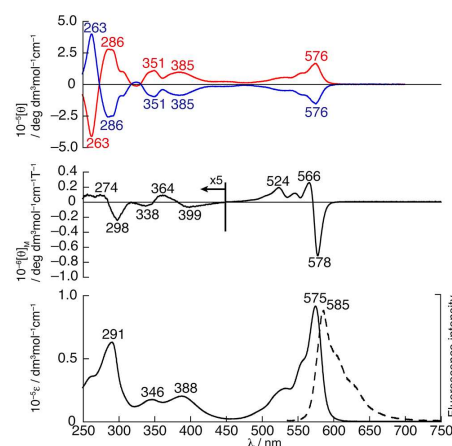


Fig. 30. UV/Vis (bottom, solid line), fluorescence (bottom, dashed line), and MCD (middle) spectra of **36**, and CD (top) spectra of **36Fr1** (blue) and **36Fr2** (red) in CHCl_3 (Reproduced from Ref. 71 with permission from ACS).

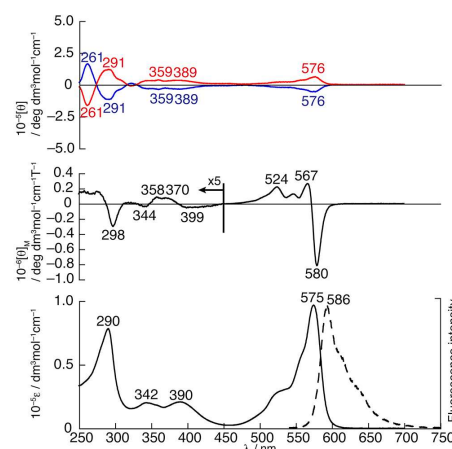


Fig. 31. UV/Vis (bottom, solid line), fluorescence (bottom, dashed line), and MCD (middle) spectra of **37**, and CD (top) spectra of **37Fr1** (blue) and **37Fr2** (red) in CHCl_3 (Reproduced from Ref. 71 with permission from ACS).

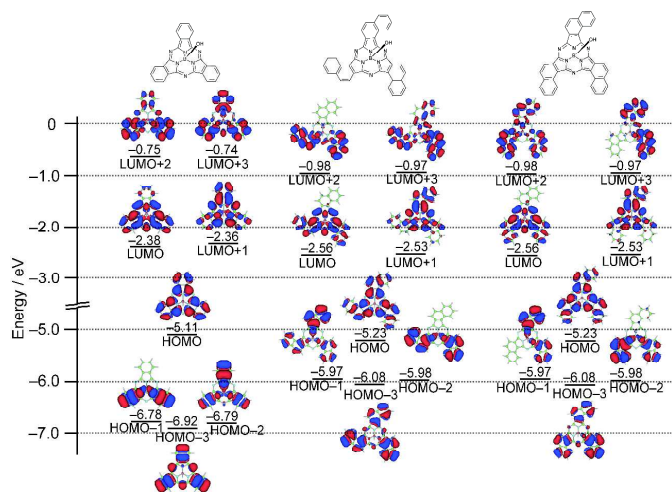


Fig. 32. Partial frontier MO diagrams of reference SubPc (left), **36** (middle), and **37** (right). The model structures used for the calculation are shown above (Reproduced from Ref. 71 with permission from ACS).

All of the enantiomers of **36** and **37** were successfully separated by HPLC equipped with a chiral column, and two fractions were obtained, among which the first and second fractions are referred to as **36Fr1** and **37Fr1**, and **36Fr2** and **37Fr2**, respectively. In the circular dichroism (CD) spectra, **36Fr1** and **37Fr1** showed a negative sign between 275 and 600 nm and a positive sign in the higher energy region, whereas the second fractions showed mirror-imaged positive and negative signs in the corresponding regions (Fig. 30 and 31). Compared to the CD signals between the same fractions of the different diastereomers, the intensities of the CD signals of the C_3 -symmetric diastereomers were almost three-times larger than those of the C_1 -symmetric diastereomers. Based on band deconvolution analysis of the absorption, CD, and MCD spectra in the Q band region,³⁷ this variation was ascribed to a decrease in the transition magnetic dipole moments, since the rotational strengths, which relate to the CD intensities, are given by the imaginary part of the scalar product of the transition electric dipole moment and transition magnetic dipole moment.^{25,73} Considering that circularly redistribution of charges in transitions generates transition magnetic dipole moments, it appeared plausible that one oppositely arranged naphthalene moiety in the structure of **37** reduces it to one-third of those of **36**.

The relationship between absolute structure and CD spectra was determined by the X-ray crystallographic analysis of **38Fr1** (Fig. 29), which was the first eluted fraction of the C_3 -symmetric diastereomer with a *p*-bromophenoxy axial ligand, based on the Bijvoet method.⁷² **38Fr1** exhibited a clockwise arrangement of the naphthalene moieties when viewed from the top of the cone structure of SubPc. This result was consistent with the theoretical CD calculations based on the TDDFT method. As the same structure-chirality relationship is also true for the C_1 -symmetric diastereomers, and the axial ligands have an only negligible influence on the chirality of the molecule, it can be concluded that the positive and negative CD signs in the

Q band region are, therefore, indicative of the anti-clockwise isomers and clockwise isomers, respectively (Fig. 33). Although this structure-chirality relationship cannot be directly applied to other chiral SubPc systems, it is anticipated that further investigation into the relationships between the structure and the direction of the transition electric dipole moment and transition magnetic dipole moment will give us a general rule for the signs of the CD spectra of the inherently chiral SubPcs.

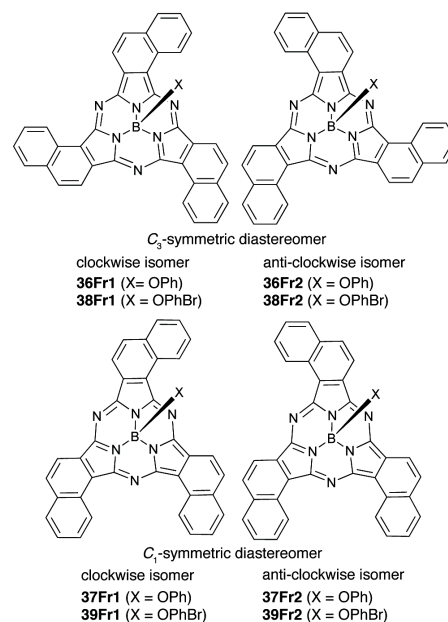


Fig. 33. Structure-chirality relationship of 1,2-SubNcs.

Concluding remarks

In this feature article, the recent progress in the synthesis of structurally-modified SubPc including modification of the bridging unit, core-modification, and exterior-modification, promoted by the authors is described. Since the discovery of SubPc by Meller and Ossko in 1972,³ many unique properties have been anticipated from the bowl-shaped C_3 -symmetric structure and 14π -electron conjugated system, such as possible tuning of the absorption and fluorescence properties, aromaticity in the bowl-shaped molecules, convex-concave interaction, bowl-chirality, and so on. The synthetic strategy based on the modification of the bridging unit enabled tuning of the optical properties due to the expansion of the conjugated system. The core-modification strategy led to tuning of the optical properties without changing of the number of π -electrons in the conjugation as well as dynamic molecular motion to probe differences in the aromaticity arising from the convex and concave surfaces. Finally the exterior-modification demonstrated arrangement of the functional units in a symmetric manner using the geometry of SubPc, convex-concave interactions with fullerenes, which results in the unique one-dimensional arrangement in the cocrystallate, and bowl-chirality with unambiguous elucidation of the structure-chirality relationship. The possible structural modifications

surveyed in this feature article, therefore, demonstrated and realized most of the expected properties of SubPc. Taking into consideration the fact that SubPc has become an important class of functional molecules in the fields of the optoelectronics and molecular electronics,^{1,5-9} this feature article will provide a future prospect for the functional molecular design based on the structure of SubPc. Furthermore the authors' group will continue to pioneer this field, and their work will be reported in due course elsewhere in the near future.

Acknowledgements

The contributions of the authors described herein were partly supported by a Grant-in-Aids for Scientific Research on Innovative Areas ("Emergence of Highly Elaborated π -Space and Its Function" (No. 20108001) and "New Polymeric Materials Based on Element-Blocks (No. 25102503)) from the Ministry of Education, Culture, Sports, Science, and Technology (MEXT), Grant-in-Aids for Young Scientists B (No. 20750025), for Scientific Research (C) (No. 23550040) and (B) (No. 23350095), and for Challenging Exploratory Research (No. 25610019) from Japan Society for the Promotion of Science (JSPS), a Grant-in-Aid for bilateral program promoted by JSPS and National Research Foundation (NRF) of South Africa, Tokuyama Science Foundation, Iwatani Naoji Foundation, and the Exploratory Research Program for Young Scientists from Tohoku University.

Notes and references

^a Department of Chemistry, Graduate School of Science, Tohoku University, Sendai 980-8578, Japan Fax: (+81)-22-795-7728 E-mail: ssoji@m.tohoku.ac.jp, nagaok@m.tohoku.ac.jp

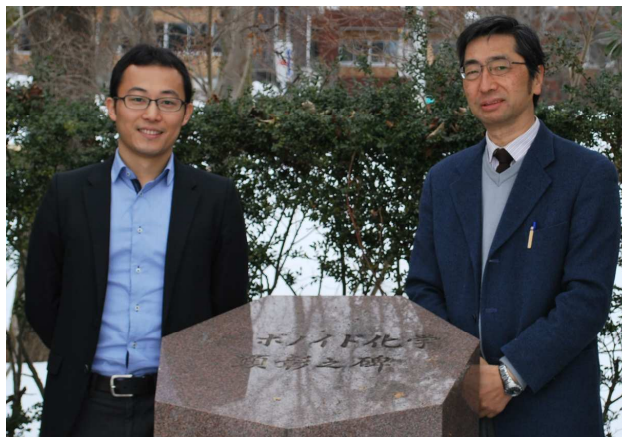
- (a) C. G. Claessens, D. González-Rodríguez, M. S. Rodríguez-Morgade, A. Medina and T. Torres, *Chem. Rev.*, 2014, DOI: 10.1021/cr400088w; (b) C. G. Claessens, D. González-Rodríguez and T. Torres, *Chem. Rev.*, 2002, **102**, 835-853 and references therein.
- (a) J. L. Sessler and S. J. Weighorn, *Expanded, Contracted & Isomeric Porphyrins*, Pergamon, Oxford, 1997; (b) J. L. Sessler, A. Gebauer and S. J. Weighorn, *The Porphyrin Handbook*, ed. K. M. Kadish, K. M. Smith and R. Guilard, Academic Press, San Diego, 2003, vol. 2, Chap. 9, pp. 55-124.
- A. Meller and A. Ossko, *Monatsh. Chem.*, 1972, **103**, 150-155.
- Recently highly fluorescent SubPcs with a fluorescence quantum yield up to 0.95 were reported, see: N. Shibata, B. Das, E. Tokunaga, M. Shiro and N. Kobayashi, *Chem. Eur. J.*, 2010, **16**, 7554-7562.
- (a) G. de la Torre, P. Vázquez, F. Agullo-Lopez and T. Torres, *J. Mater. Chem.*, 1998, **8**, 1671-1683; (b) G. de la Torre, P. Vázquez, F. Agullo-Lopez and T. Torres, *Chem. Rev.*, 2004, **104**, 3723-3750.
- (a) C. K. Renshaw, X. Xu and S. R. Forrest, *Org. Electron.*, 2010, **11**, 175-178; (b) T. Yasuda and T. Tsutsui, *Mol. Cryst. Liq. Cryst.*, 2007, **462**, 3-9.
- (a) Y.-H. Chen, J.-H. Chang, G.-R. Lee, I.-W. Wu, J.-H. Fang, C.-I. Wu and T.-W. Pi, *Appl. Phys. Lett.*, 2009, **95**, 133302; (b) M. G. Helander, G. E. Morse, J. Qiu, J. S. Castrucci, T. P. Bender and Z. H. Lu, *ACS Appl. Mater. Interfaces*, 2010, **2**, 3147-3152; (c) G. E. Morse, M. G. Helander, J. F. Maka, Z. H. Lu and T. P. Bender, *ACS Appl. Mater. Interfaces*, 2010, **2**, 1934-1944.
- Y. Wang, D. H. Gu and F. X. Gan, *Phys. Status Solidi A*, 2001, **186**, 71-77.
- K. L. Mutolo, E. I. Mayo, B. P. Rand, S. R. Forrest and M. E. Thompson, *J. Am. Chem. Soc.*, 2006, **128**, 8108-8109.
- (a) Y. Inokuma, J. H. Kwon, T. K. Ahn, M. C. Yoon, D. Kim and A. Osuka, *Angew. Chem. Int. Ed.*, 2006, **45**, 961-964; (b) Y. Inokuma, Z. S. Yoon, D. Kim and A. Osuka, *J. Am. Chem. Soc.*, 2007, **129**, 4747-4761; (c) A. Osuka, E. Tsurumaki and T. Tanaka, *Bull. Chem. Soc. Jpn.*, 2011, **84**, 679-697.
- R. Myśliwski, L. Latos-Grażyński, L. Szterenberga and T. Lis, *Angew. Chem. Int. Ed.*, 2006, **45**, 3670-3674.
- Z. L. Xue, Z. Shen, J. Mack, D. Kuzuhara, H. Yamada, T. Okujima, N. Ono, X. Z. You and N. Kobayashi, *J. Am. Chem. Soc.*, 2008, **130**, 16478-16479.
- (a) Y. Takeuchi, A. Matsuda and N. Kobayashi, *J. Am. Chem. Soc.*, 2007, **129**, 8271-8281; (b) N. Kobayashi, Y. Takeuchi and A. Matsuda, *Angew. Chem. Int. Ed.*, 2007, **46**, 758-760.
- S. Higashibayashi and H. Sakurai, *J. Am. Chem. Soc.*, 2008, **130**, 8592-8593.
- D. Kuzuhara, H. Yamada, Z. L. Xue, T. Okujima, S. Mori, Z. Shen and H. Uno, *Chem. Commun.*, 2011, **47**, 722-724.
- K. S. Anju, S. Ramakrishnan and A. Srinivasan, *Org. Lett.*, 2011, **13**, 2498-2501.
- (a) M. Kitano, S. Hayashi, T. Tanaka, H. Yorimitsu, N. Aratani and A. Osuka, *Angew. Chem. Int. Ed.*, 2012, **51**, 5593-5597; (b) T. Tanaka, M. Kitano, S. Hayashi, N. Aratani and A. Osuka, *Org. Lett.*, 2012, **14**, 2694-2697.
- (a) Y. J. Yang and Z. M. Su, *Int. J. Quantum. Chem.*, 2005, **103**, 54-59; (b) Y. Yang, *Chem. Phys. Lett.*, 2011, **511**, 51-56.
- A. MacCragh and W. S. Koski, *J. Am. Chem. Soc.*, 1965, **87**, 2496-2497.
- E. W. Y. Wong, A. Miura, M. D. Wright, Q. He, C. J. Walsby, S. Shimizu, N. Kobayashi and D. B. Leznoff, *Chem. Eur. J.*, 2012, **18**, 12404-12410.
- B. Franck and A. Nonn, *Angew. Chem. Int. Ed. Engl.*, 1995, **34**, 1795-1811.
- (a) M. Gouterman, *J. Chem. Phys.*, 1959, **30**, 1139-1161; (b) M. Gouterman, *J. Mol. Spectrosc.*, 1961, **6**, 138-163.
- M. J. Stillman and T. Nyokong, ed. C. C. Leznoff and A. B. P. Lever, Wiley-VCH, New York, 1989-1996, vol. 1, Chap. 3, pp. 133-289.
- (a) J. Mack, M. J. Stillman and N. Kobayashi, *Coord. Chem. Rev.*, 2007, **251**, 429-453; (b) J. Mack, N. Kobayashi and Z. Shen, *Handbook of Porphyrin Science*, World Scientific, Singapore, 2012, vol. 23, Chap. 109, pp. 281-371.
- N. Kobayashi, A. Muranaka and J. Mack, *Circular Dichroism and Magnetic Circular Dichroism Spectroscopy for Organic Chemists*, Royal Society of Chemistry, UK, 2012.
- J. Michl, *J. Am. Chem. Soc.*, 1978, **100**, 6801-6811.
- (a) T. D. Lash, *Handbook of Porphyrin Science*, ed. K. M. Kadish, K. M. Smith and R. Guilard, World Scientific Publishing, Singapore, 2012, vol. 16, Chap. 74, pp. 1-329; (b) M. Pawlicki and L. Latos-Grażyński, *Handbook of Porphyrin Science*, ed. K. M. Kadish, K. M. Smith and R. Guilard, World Scientific Publishing, Singapore, 2010,

- vol. 2, Chap. 8, pp. 103-192; (c) M. Stępień and L. Latos-Grażyński, *Acc. Chem. Res.*, 2005, **38**, 88-98.
28. (a) J. A. Elvidge and R. P. Linstead, *J. Chem. Soc.*, 1952, 5008-5012; (b) P. F. Clark, J. A. Elvidge and R. P. Linstead, *J. Chem. Soc.*, 1954, 2490-2497.
29. (a) F. Fernandez-Lazaro, T. Torres, B. Hauschel and M. Hanack, *Chem. Rev.*, 1998, **98**, 563-575; (b) M. S. Rodríguez-Morgade, G. de la Torre and T. Torres, *The Porphyrin Handbook*, ed. K. M. Kadish, K. M. Smith and R. Guilard, Academic Press, San Diego, 2003, vol. 15, Chap. 99, pp. 125-160.
30. C. J. Ziegler, *Handbook of Porphyrin Science*, ed. K. M. Kadish, K. M. Smith and R. Guilard, World Scientific Publishing, Singapore, 2012, vol. 17, Chap. 77, pp. 114-238.
31. (a) N. Kobayashi, S. Inagaki and V. Nemykin, *Angew. Chem. Int. Ed.*, 2001, **40**, 2710-2712; (b) S. Shimizu, Y. Sato and N. Kobayashi, *Chem. Lett.*, 2012, **41**, 702-704.
32. (a) M. K. Islyaiquin, E. A. Danilova, L. D. Yagodarova, M. S. Rodríguez-Morgade and T. Torres, *Org. Lett.* 2001, **3**, 2153-2156; (b) O. N. Trukhina, M. S. Rodríguez-Morgade, S. Wolfrum, E. Caballero, N. Snejko, E. A. Danilova, E. Gutiérrez-Puebla, M. K. Islyaiquin, D. M. Guldi and T. Torres, *J. Am. Chem. Soc.*, 2010, **132**, 12991-12999.
33. A. Muranaka, S. Ohira, D. Hashizume, H. Koshino, F. Kyotani, M. Hirayama and M. Uchiyama, *J. Am. Chem. Soc.*, 2012, **134**, 190-193.
34. (a) S. Shimizu, H. Zhu and N. Kobayashi, *Chem. Eur. J.*, 2010, **16**, 11151-11159; (b) S. Shimizu, H. Zhu and N. Kobayashi, *Chem. Commun.*, 2011, **47**, 3072-3074; (c) S. Shimizu, K. Uemura, H. Zhu and N. Kobayashi, *Tetrahedron Lett.*, 2012, **53**, 579-581.
35. H. Zhu, S. Shimizu and N. Kobayashi, *Angew. Chem. Int. Ed.*, 2010, **49**, 8000-8003.
36. S. Shimizu, S. Nakano, A. Kojima and N. Kobayashi, *Angew. Chem. Int. Ed.*, 2014, **53**, 2408-2412.
37. (a) W. R. Browett and M. J. Stillman, *Comput. Chem.*, 1987, **11**, 241-250; (b) N. Kobayashi, T. Fukuda and D. Lelievre, *Inorg. Chem.*, 2000, **39**, 3632-3637.
38. J. R. Stork, R. J. Potucek, W. S. Durfee and B. C. Noll, *Tetrahedron Lett.*, 1999, **40**, 8055-8058.
39. (a) N. Kobayashi, J. Mack, K. Ishii and M. J. Stillman, *Inorg. Chem.*, 2002, **41**, 5350-5363; (b) N. Kobayashi, H. Miwa and V. N. Nemykin, *J. Am. Chem. Soc.*, 2002, **124**, 8007-8020; (c) N. Kobayashi and T. Fukuda, *J. Am. Chem. Soc.*, 2002, **124**, 8021-8034; (d) H. Miwa, K. Ishii and N. Kobayashi, *Chem. Eur. J.*, 2004, **10**, 4422-4435; (e) T. Fukuda, E. A. Makarova, E. A. Luk'yanets and N. Kobayashi, *Chem. Eur. J.*, 2004, **10**, 117-133.
40. M. S. Rodríguez-Morgade, C. G. Claessens, A. Medina, D. González-Rodríguez, E. Gutiérrez-Puebla, A. Monge, I. Alkorta, J. Elguero and T. Torres, *Chem. Eur. J.*, 2008, **14**, 1342-1350.
41. Similar rotation barrier energy was reported for propyl-bridged biphenyl derivatives, see: J. Rotzler, H. Gsellinger, M. Neuburger, D. Vonlanthen, D. Häussinger and M. Mayor, *Org. Biomol. Chem.*, 2011, **9**, 86-91.
42. (a) D. González-Rodríguez, E. Carbonell, D. M. Guldi and T. Torres, *Angew. Chem. Int. Ed.*, 2009, **48**, 8032-8036; (b) D. González-Rodríguez, E. Carbonell, G. D. Rojas, C. A. Castellanos, D. M. Guldi and T. Torres, *J. Am. Chem. Soc.*, 2010, **132**, 16488-16500; (c) R. S. Iglesias, C. G. Claessens, T. Torres, G. M. A. Rahman and D. M. Guldi, *Chem. Commun.*, 2005, 2113-2115; (d) D. González-Rodríguez, T. Torres, D. M. Guldi, J. Rivera, M. A. Herranz and L. Echegoyen, *J. Am. Chem. Soc.*, 2004, **126**, 6301-6313; (e) D. González-Rodríguez, T. Torres, M. A. Herranz, L. Echegoyen, E. Carbonell and D. M. Guldi, *Chem. Eur. J.*, 2008, **14**, 7670-7679.
43. E. Caballero, J. Fernández-Ariza, V. M. Lynch, C. Romero-Nieto, M. S. Rodríguez-Morgade, J. L. Sessler, D. M. Guldi and T. Torres, *Angew. Chem. Int. Ed.*, 2012, **51**, 11337-11342.
44. M. A. Petrukhina and L. T. Scott, *Fragments of Fullerenes and Carbon Nanotubes: Designed Synthesis, Unusual Reactions, and Coordination Chemistry*, Wiley, 2011.
45. (a) T. Fukuda and N. Kobayashi, *Dalton Trans.*, 2008, 4685-4704; (b) E. A. Makarova, E. V. Dzyulina, T. Fukuda, H. Kaneko, N. Hashimoto, Y. Kikukawa, N. Kobayashi and E. A. Luk'yanets, *Inorg. Chem.*, 2009, **48**, 164-173; (c) E. A. Makarova, T. Fukuda, E. A. Luk'yanets and N. Kobayashi, *Chem. Eur. J.*, 2005, **11**, 1235-1250; (d) H. Miwa, E. A. Makarova, K. Ishii, E. A. Luk'yanets and N. Kobayashi, *Chem. Eur. J.*, 2002, **8**, 1082-1090.
46. (a) J. Rauschnabel and M. Hanack, *Tetrahedron Lett.*, 1995, **36**, 1629-1632; (b) C. D. Zyskowski and V. O. Kennedy, *J. Porphyrins Phthalocyanines*, 2000, **4**, 707-712; (c) S. Nonell, N. Rubio, B. del Rey and T. Torres, *J. Chem. Soc., Perkin Trans. 2*, 2000, **6**, 1091-1094.
47. (a) M. S. Rodríguez-Morgade, S. Esperanza, T. Torres and J. Barbera, *Chem. Eur. J.*, 2005, **11**, 354-360; (b) J. R. Stork, J. J. Brewer, T. Fukuda, J. P. Fitzgerald, G. T. Yee, A. Y. Nazarenko, N. Kobayashi and W. S. Durfee, *Inorg. Chem.*, 2006, **45**, 6148-6151.
48. (a) T. Fukuda, J. R. Stork, R. J. Potucek, M. M. Olmstead, B. C. Noll, N. Kobayashi and W. S. Durfee, *Angew. Chem. Int. Ed.*, 2002, **41**, 2565-2568; (b) C. G. Claessens and T. Torres, *Angew. Chem. Int. Ed.*, 2002, **41**, 2561-2565.
49. R. S. Iglesias, C. G. Claessens, T. Torres, M. A. Herranz, V. R. Ferro and J. M. G. de la Vega, *J. Org. Chem.*, 2007, **72**, 2967-2977.
50. G. D. Dorough and F. M. Huennekens, *J. Am. Chem. Soc.*, 1952, **74**, 3974-3976.
51. C. Brückner, L. Samankumara and J. Ogikubo, *Handbook of Porphyrin Science*, ed. K. M. Kadish, K. M. Smith and R. Guilard, World Scientific Publishing, Singapore, 2012, vol. 17, Chap. 76, pp. 1-112.
52. E. Tsurumaki, S. Saito, K. S. Kim, J. M. Lim, Y. Inokuma, D. Kim and A. Osuka, *J. Am. Chem. Soc.*, 2008, **130**, 438-439.
53. S. Hayashi, E. Tsurumaki, Y. Inokuma, P. Kim, Y. M. Sung, D. Kim and A. Osuka, *J. Am. Chem. Soc.*, 2011, **133**, 4254-4256.
54. S. Shimizu, T. Otaki, Y. Yamazaki and N. Kobayashi, *Chem. Commun.*, 2012, **48**, 4100-4102.
55. J. L. Segura and N. Martin, *Angew. Chem. Int. Ed.*, 2001, **40**, 1372-1409 and references therein.
56. (a) M. A. Blower, M. R. Bryce and W. Devonport, *Adv. Mater.*, 1996, **8**, 63-65; (b) C. Farren, C. A. Christensen, S. FitzGerald, M. R. Bryce and A. Beeby, *J. Org. Chem.*, 2002, **67**, 9130-9139; (c) M. J. Cook, G. Cooke and A. Jafari-Fini, *Chem. Commun.*, 1996, 1925-1926; (d) C. Wang, M. R. Bryce, A. S. Batsanov, C. F. Stanley, A. Beeby and J. A. K. Howard, *J. Chem. Soc., Perkin Trans. 2*, 1997, 1671-1678; (e) H. Yingyu and S. Yongjia, *J. Heterocycl. Chem.*, 2002, **39**, 1071-1075; (f) C. Loosli, C. Jia, S.-X. Liu, M. Haas, M. Dias, E. Levillain, A. Neels, G. Labat, A. Hauser and S. Decurtins, *J.*

- Org. Chem.*, 2005, **70**, 4988-4992; (g) J. Sly, P. Kasák, E. Gomar-Nadal, C. Rovira, L. Górriz, P. Thordarson, D. B. Amabilino, A. E. Rowan and R. J. M. Nolte, *Chem Commun*, 2005, 1255-1257; (h) T. Kimura, *Heterocycles*, 2013, **87**, 245-274.
57. (a) J. Becher, T. Brimert, J. O. Jeppesen, J. Z. Pedersen, R. Zubarev, T. Bjørnholm, N. Reitzel, T. R. Jensen, K. Kjaer and E. Levillain, *Angew. Chem. Int. Ed.*, 2001, **40**, 2497-2500; (b) H. Li, J. O. Jeppesen, E. Levillain and J. Becher, *Chem. Commun.*, 2003, 846-847; (c) K. A. Nielsen, E. Levillain, V. M. Lynch, J. L. Sessler and J. O. Jeppesen, *Chem. Eur. J.*, 2009, **15**, 506-516; (d) A. Jana, M. Ishida, K. Kwak, Y. M. Sung, D. S. Kim, V. M. Lynch, D. Lee, D. Kim and J. L. Sessler, *Chem. Eur. J.*, 2013, **19**, 338-349.
58. S. Shimizu, Y. Yamazaki and N. Kobayashi, *Chem. Eur. J.*, 2013, **19**, 7324-7327.
59. (a) A. Kaito, T. Nozawa, T. Yamamoto, M. Hatano and Y. Oorii, *Chem. Phys. Lett.*, 1977, **52**, 154-160; (b) A. Tajiri and J. Winkler, *Z. Naturforsch., A: Phys. Sci.* 1983, **38**, 1263-1269.
60. (a) V. M. Tsefrikas and L. T. Scott, *Chem. Rev.*, 2006, **106**, 4868-4884; (b) Y. T. Wu and J. S. Siegel, *Chem. Rev.*, 2006, **106**, 4843-4867.
61. H. Sakurai, T. Daiko and T. Hirao, *Science*, 2003, **301**, 1878-1878.
62. K. Kawasumi, Q. Zhang, Y. Segawa, L. T. Scott and K. Itami, *Nature Chem.*, 2013, **5**, 739-744.
63. (a) I. Sánchez-Molina, B. Grimm, R. M. Krick Calderon, C. G. Claessens, D. M. Guldi and T. Torres, *J. Am. Chem. Soc.*, 2013, **135**, 10503-10511; (b) C. G. Claessens and T. Torres, *Chem. Commun.*, 2004, 1298-1299.
64. I. Sánchez-Molina, C. G. Claessens, B. Grimm, D. M. Guldi and T. Torres, *Chem. Science*, 2013, **4**, 1338-1344.
65. S. Shimizu, S. Nakano, T. Hosoya and N. Kobayashi, *Chem. Commun.*, 2011, **47**, 316-318.
66. For the absorption and MCD spectra of **32**, see Ref. 65.
67. P. D. W. Boyd and C. A. Reed, *Acc. Chem. Res.*, 2005, **38**, 235-242.
68. C. G. Claessens and T. Torres, *Tetrahedron Lett.*, 2000, **41**, 6361-6365.
69. N. Kobayashi and T. Nonomura, *Tetrahedron Lett.*, 2002, **43**, 4253-4255.
70. (a) M. Hanack, G. Renz, J. Strahle and S. Schmid, *J. Org. Chem.*, 1991, **56**, 3501-3509; (b) V. M. Negrimovskii, M. Bouvet, E. A. Luk'yanets and J. Simon, *J. Porphyrins Phthalocyanines*, 2000, **4**, 248-255; (c) E. H. Gacho, T. Naito, T. Inabe, T. Fukuda and N. Kobayashi, *Chem. Lett.*, 2001, 260-261; (d) E. H. Gacho, H. Imai, R. Tsunashima, T. Naito, T. Inabe and N. Kobayashi, *Inorg. Chem.*, 2006, **45**, 4170-4176.
71. S. Shimizu, A. Miura, S. Khene, T. Nyokong and N. Kobayashi, *J. Am. Chem. Soc.*, 2011, **133**, 17322-17328.
72. H. D. Flack and G. Bernardinelli, *J. Appl. Crystallogr.*, 2000, **33**, 1143-1148.
73. A. Roger and B. Norden, *Circular Dichroism and Linear Dichroism*, Oxford University Press, Oxford, 1997.

Author Profile: Soji Shimizu was born in Kyoto, Japan, in 1979. He graduated from Kyoto University in 2002, and obtained his PhD there under the supervision of Professor Atsuhiko Osuka in 2007 for his research on the syntheses and properties of expanded porphyrins. During his PhD studies, he made a short stay in the group of Professor Jonathan L. Sessler, the University of Texas at Austin in 2005. In 2006, he was appointed as an assistant professor at the Department of Chemistry, Graduate School of Science, Tohoku University and started his academic carrier in the group of Professor Nagao Kobayashi in the field of phthalocyanine chemistry. He was, then, promoted to a lecturer there in 2010. His research interests cover the synthesis of conjugated molecules with novel structures and their optical and electrochemical properties.

Nagao Kobayashi received a Dr. of Sc. degree from Tohoku University for his study on the magnetic circular dichroism spectroscopy of peroxidase and catalase. In 1986 he obtained a Dr. of Pharmacy degree based on a study of the electrocatalytic reduction of oxygen by water-soluble porphyrins and phthalocyanines. Since 1995, he has been a full professor at the Department of Chemistry, Graduate School of Science, Tohoku University. His research interests cover many different areas of porphyrin and phthalocyanine chemistry with a strong focus on synthesis, electrochemistry and optical spectroscopy. The CD and MCD spectroscopy of porphyrinoids is a key area of expertise. He received a Chemical Society of Japan Award for Creative Work in the chemistry of giant aromatic molecules in 2007.



Graphical abstract

